4-20-2020

Meaning in the noise: Neural signal variability in major depressive disorder

Sally M. Pessin
University of Missouri-St. Louis, smptb3@mail.umsl.edu

Meaning in the noise:

Neural signal variability in major depressive disorder

Sally M. Pessin

B.S. Psychology, Truman State University, 2017

A Thesis Submitted to The Graduate School at the University of Missouri – Saint Louis
in partial fulfillment of the requirements for the degree
Master of Arts in Psychology
with an emphasis in Behavioral Neuroscience

May 2020

Advisory Committee

Carissa L. Philippi, Ph.D.
Chairperson

Sandra Langeslag, Ph.D.

John Meriac, Ph.D.

Abstract

Clinical research has revealed aberrant activity and connectivity in default mode (DMN), frontoparietal (FPN), and salience (SN) network regions in major depressive disorder (MDD). Recent functional magnetic resonance imaging (fMRI) studies suggest that variability in brain activity, or blood oxygen level-dependent (BOLD) signal variability, may be an important novel predictor of psychopathology. However, to our knowledge, no studies have yet determined the relationship between resting-state BOLD signal variability and MDD nor applied BOLD signal variability features to the classification of MDD history using machine learning (ML). Thus, the current study had three aims: (*i*) to investigate the differences in the voxel-wise resting-state BOLD signal variability between varying depression histories; (*ii*) to examine the relationship between depressive symptom severity and resting-state BOLD signal variability; (*iii*) to explore the capability of resting-state BOLD signal variability to classify individuals by depression history. Using resting-state neuroimaging data for 79 women collected as a part of a larger NIH R01-funded study, we conducted (*i*) a one-way between-subjects ANCOVA, (*ii*) a multivariate multiple regression, and (*iii*) applied BOLD signal variability and average BOLD signal features to a supervised ML model. First, results indicated that individuals with any history of depression had significantly decreased BOLD signal variability in the left and right cerebellum and right parietal cortex in comparison to those with no depression history ($p_{FWE} < .05$). Second, and consistent with the results for depression history, depression severity was associated with reduced BOLD signal variability in the cerebellum. Lastly, a random forest model classified participant depression history with 76% accuracy, with BOLD signal variability features showing

greater discriminative power than average BOLD signal features. These findings provide support for resting-state BOLD signal variability as a novel marker of neural dysfunction and implicate decreased neural signal variability as a neurobiological mechanism of depression.

Keywords: major depressive disorder, neural signal variability, BOLD variability, default mode network, salience network, frontoparietal network, machine learning

Meaning in the noise: Neural signal variability in major depressive disorder

Major depressive disorder (MDD) is a debilitating psychiatric condition and leading cause of disability, affecting more than 320 million of the global population (Ferrari et al., 2013; World Health Organization). MDD is characterized by consistent depressed mood and fatigue, feelings of worthlessness, and an inability to feel pleasure (American Psychiatric Association, 2013). Due to its prevalence, it is critical to explore the neurobiological bases of MDD as these mechanisms may provide biomarkers for early intervention and treatment.

Neural Dysfunction in MDD

Several studies in the past two decades seeking to elucidate the neurobiological mechanisms of MDD have utilized functional magnetic resonance imaging (fMRI). Functional MRI measures blood oxygen level-dependent (BOLD) signal through the detection of changes in blood flow and the relative concentration of oxygenated to deoxygenated hemoglobin. With BOLD signal, it is possible to infer where neural activity is occurring in response to a task (task-based) or during the absence of a task (resting-state; Damoiseaux & Greicius, 2009). In addition to simply looking at topographical activation in the brain, it is possible with fMRI to view the brain as an efficient network of functional communication. An example of this in practice is seed-based functional connectivity (FC). Using this method, the BOLD time course of a particular region (i.e., seed) may be selected and correlated to the BOLD time course of all other regions of the brain. The results of this analysis highlight areas of the brain that activate in conjunction with as well as areas that are inversely related to the initial region of interest (ROI; van den Heuvel & Hulshoff Pol, 2010). This method, consequently,

indicates networks of regions that are functionally related and can be examined in relation to psychopathology.

In general, fMRI research on the pathophysiology of depression examines regions and networks of aberrant activity both at rest and in response to a task. Evidence from this research suggests that the activity of emotion processing regions, such as the limbic-cortical-striatal-pallidal-thalamic circuit (LCSPT), is related to mood disorders (Ongür et al., 2003; Phillips et al., 2003). Consisting of the orbital and medial prefrontal cortex, limbic regions, striatum, pallidum, and thalamus, the LCSPT was first implicated in depression in neurodegenerative disease and lesion studies (Folstein et al., 1985). In reviewing later neuroimaging studies, Drevets, Price, and Furey (2008) emphasized the increase in medial prefrontal cortex (mPFC) activity and resulting disinhibition of activity in the amygdala contribute to depressive symptoms. Similarly, individuals with MDD presented increased connectivity between these regions at rest, particularly with the subgenual anterior cingulate cortex (ACC; Greicius et al., 2007).

A network consisting of some LCSPT regions has been consistently related in fMRI research to depressive symptoms and depression severity: the default mode network (DMN). This network has primarily been associated with self-referential processing, and its hyperactivity has been implicated in thoughts of worthlessness, rumination, and self-blame in depression (Berman et al., 2011; Kaiser, Andrews-Hanna, Wager, & Pizzagalli, 2015; Sheline et al., 2009; Whitfield-Gabrieli & Ford, 2012; Zhu et al., 2012). The core regions of this network include the mPFC, posterior cingulate cortex (PCC), retrosplenial cortex, and the left and right inferior parietal lobule (IPL; Greicius et al., 2007; Whitfield-Gabrieli & Ford, 2012; Williams, 2017). Berman et al. (2011) found

individuals with depression had greater connectivity between the PCC, mPFC, and subgenual ACC in comparison to healthy individuals. There was a comparable finding in treatment naive MDD patients where there was greater FC between the dorsal and ventral mPFC and ventral ACC than healthy controls (Zhu et al., 2012). Likewise, Whitfield-Gabrieli and Ford (2012) reiterated there is hyperactivity within and hyperconnectivity between these regions for individuals with depression both in resting-state and task-based studies.

However, the increased activity within the DMN has been coupled with the reduced and altered BOLD signal in other regions and networks. It has been argued since the DMN primarily processes internal and self-referential thoughts, this comes at a cost to other networks concerned with attentional processes, external stimuli, and cognitively demanding tasks, such as the frontoparietal network (FPN) and salience network (SN; Pizzagalli, 2011; Whitfield-Gabrieli & Ford, 2012). The FPN comprises the dorsolateral PFC (dlPFC) and intraparietal sulcus (IPS) and has shown lower inverse correlations with the DMN in individuals with depression in comparison to healthy individuals (Mulders, van Eijndhoven, Schene, Beckmann, & Tendolkar, 2015; Pizzagalli, 2011). Altered connectivity in depression was also found between the DMN and the amygdala and anterior insula of the SN (Manoliu et al., 2014; Mulders et al., 2015; Ramasubbu et al., 2014). Moreover, reductions in connectivity between regions within the FPN have been associated with depression (Alexopoulos et al., 2012; Liston et al., 2014) and SN (Ramasubbu et al., 2014; Tahmasian et al., 2013).

Based on these findings, there is a distinct association between depression and the functional networks of the brain at rest. This is evident in the heightened activity and

connectivity within the DMN, as well as the decreased and altered connectivity between the DMN and FPN and DMN and SN, respectively. However, most neuroimaging studies examining the DMN, FPN, and SN have utilized average BOLD signal, so it remains unclear how modeling higher-order measures of neural activity (i.e., variability) would characterize the association between depression and these networks at rest.

Brain Signal Variability

As an alternative to measures of activity and connectivity as described above that utilize the average BOLD signal, recent studies with a predominant focus in aging have explored BOLD signal variability as a novel tool for examining individual differences in resting-state activity. It was posited from this research that variability appeared to have an "optimal" level for functioning, and this was a mechanism of network integration. In other words, an optimal amount of variability tended to lead to better communication between network regions and overall better functioning systems (Garrett, Epp, Perry, & Lindenberger, 2018).

Further research on stochastic resonance supports this notion, stating the addition of noise (i.e., variability) is necessary to detect some weak, resting-state signals, and too much or too little variability may hinder neural synchronization (Burzynska et al., 2015; Garrett, Kovacevic, McIntosh & Grady, 2010). Similarly, Easson and McIntosh (2019) suggested a moderate amount of variability is required for neural systems to switch from state to state, and too little variability may impede adaptation to external information in new environments. The ability of network regions to select optimal responses to new stimuli also reflects Bayesian probabilities where optimization occurs through consideration of probability before and after information integration. That is, if the signal

remained constant, there would be no new information to analyze and, therefore, no range of responses from which to select. For this reason, neural variability can be considered the neurobiological mechanism of adaptability (Beck et al., 2008; Ma, Beck, Latham, & Pouget, 2006).

Measuring variability has been operationalized as the standard deviation (SD) or fractional SD (fSD) of BOLD signal, the mean squared successive differences of BOLD signal, amplitude of low frequency fluctuations (ALFF), and fractional ALFF (fALFF). These measures of neural variability were initially investigated in relation to age (Burzynska et al., 2015; Garrett et al., 2010; Garrett, Kovacevic, McIntosh & Grady, 2011; Grady & Garrett, 2014; Nomi, Bolt, Ezie, Uddin, & Heller, 2017); however, subsequent studies have investigated these measures in relation to psychiatric disorders.

Neural Variability as a Neurobiological Marker of Disorder

Subsequent research examined suboptimal variability patterns as an indicator of various psychiatric, developmental, and neurodegenerative conditions, such as bipolar disorder (BD; Kebets et al., 2018; Martino et al., 2016), temperament (Conio et al., 2019), attention-deficit hyperactivity disorder (Nomi et al., 2018), generalized anxiety disorder (Li et al., 2019; Månsson et al., 2018), Alzheimer's disease (Scarapicchia, Mazerolle, Fisk, Ritchie, & Gawryluk, 2018; Zhang et al., 2016), and autism (Easson & McIntosh, 2019).

In a task-based study where participants passively viewed emotionally salient film clips, individuals with the melancholic subtype of MDD presented decreased BOLD signal variability within the ventral mPFC in comparison to healthy controls (Guo, Nguyen, Hyett, Parker, & Breakspear, 2015). While the mPFC is primarily associated

with the DMN, the ventral mPFC has also been implicated in reward and threat appraisal and decision making (Williams, 2017). Thus, this reduction in BOLD signal variability for individuals with melancholic-MDD in response to viewing an emotional film clip may indicate an inability to switch mental states (Guo et al., 2015). This supports the notion that too little neural variability may consequently hinder adaptation to external stimuli (Easson & McIntosh, 2019).

For individuals in a depressive subgroup of BD, there were opposing patterns of variability between DMN and sensorimotor network (SMN) regions at rest. There was an increase in resting-state BOLD signal variability in DMN regions whereas regions in the SMN exhibited a decrease in variability (Martino et al., 2016). From these results, Martino et al. (2016) posited the greater likelihood of spontaneous, internally directed thoughts in the depressive subgroup of BD may be attributable to the abnormally higher variability in DMN regions. Analogous opposing patterns were found when examining the variability of a similar sample of depressed individuals with BD. Decreases in variability were observed in the occipital cortex, cerebellum, cingulate gyrus, and medial limbic regions, while there were increases in the ACC, ventral mPFC, orbitofrontal cortex, pallidum, and brainstem (Kebets et al., 2018). Affective temperaments have also been explored in relation to BOLD signal variability. Cyclothymic and depressive temperaments, characterized by emotional instability and melancholy, respectively, were previously investigated as the underpinnings of mood disorders, particularly BD (Perugi et al., 2012). Conio and colleagues (2018) investigated BOLD signal variability using fSD in association with these two temperaments and found those with a depressive

temperament had significantly decreased signal variability in SMN regions in comparison to individuals with a cyclothymic temperament.

It is clear from previous research there is altered variability in relation to depressive symptoms, and as stated previously, deviating from the "optimal" level of variability may disrupt functional network integration and adaptability. That being said, there is little literature explicitly examining BOLD signal variability as a function of MDD history and severity. Therefore, it remains possible to further explicate the relationship between BOLD signal variability and depression.

Machine Learning Methods in MDD Diagnosis

In pursuit of advancing current knowledge on the novel association between BOLD signal variability and MDD, it is also important to consider the promising opportunities offered by machine learning (ML). ML methods are increasingly being used for their ability to create computer-aided statistical models from low- and high-dimensional data, such as structural and functional MRI data (Rutledge, Chekroud, & Huys, 2019; Wade et al., 2015). In fact, the potential of these algorithms to classify patients into separate psychiatric conditions and treatment responses has been explored using behavioral, genetic, and neurobiological data (Bzdok & Meyer-Lindenberg, 2018; Patel, Khalaf, & Aizenstein, 2016).

ML methods, in essence, "learn" from empirical data to create predictive models that will later be assessed for accuracy in the prediction of new data. First, segments of data are randomly selected from the full dataset to train the predictive model and then adjusted through tuning and hyperparameters to enhance performance. Once the model is established, the algorithm is assessed on the remaining, unused data for accuracy (AUC),

sensitivity, and specificity (see Figure 1; Bzdok & Meyer-Lindenberg, 2018; Jahedi, Nasamran, Faires, Fan, & Müller, 2017; Patel, Khalaf, & Aizenstein, 2016). An ML method can be classified as either unsupervised or supervised based on the type of training used in its creation. Unsupervised learning models, such as k-means clustering and principal components analysis, explore data for relevant variables without *a priori* outcomes or response variables. In contrast, supervised models, including classification and regression, learn from data with a given discrete target variable or outcome, such as a diagnosis. Common supervised algorithms include random forests (RF), support vector machines, and logistic regression (Bzdok & Meyer-Lindenberg, 2018).

Haslam and Beck (1993) initially demonstrated the potential of ML algorithms for psychiatric diagnostic classification in using Beck Depression Inventory (BDI) item scores to classify syndromal subtypes of depression. Through the use of clustering techniques, they established four subtypes of MDD: general depressive type, melancholic type, generalized anxiety type, enervation-and-anhedonic features type. Contemporary applications have continued to examine the statistical ability of ML algorithms in using quantitative brain measurements in the prediction of diagnostic groups, similar to Haslam and Beck's original use, as well as for predicting treatment responses and outcomes (Bzdok & Meyer-Lindenberg, 2018).

Indeed, average structural and functional measures from fMRI, electroencephalograms (EEG), and diffusion tensor imaging (DTI) have been utilized in both supervised and unsupervised models as features to classify individuals by psychiatric symptoms and diagnosis (Gosnell, Fowler, & Salas, 2019; Mumtaz, Ali, Yasin, & Malik, 2018; Patel et al., 2015; Sacchet, Prasad, Foland-Ross, Thompson, &

Gotlib, 2015; Shimizu et al., 2015; Zeng et al., 2012; Zeng, Shen, Liu, & Hu, 2014). In a study comparing ML methods in late-life depression classification, a supervised alternating decision trees method outperformed other ML methods (AUC = 87.27%) when using resting-state fMRI ROIs selected from the DMN (Patel et al., 2015). Wade et al. (2015) utilized an RF classification method and found two morphological descriptors in MRI anatomical images were most accurate in differentiating individuals with MDD from healthy controls: Jacobian determinant (AUC = 89.58%) and radial distance maps (AUC = 77.08%). Similarly, an RF model achieved 75% accuracy when applied in the classification of suicidal behavior through 47 rsFC features (Gosnell et al., 2019). Through unsupervised maximum margin clustering, Zeng and colleagues (2014) established the resting-state functional connections between the subgenual and pregenual ACC provided 92.5% and 84.9% accuracy, respectively, in categorizing MDD patients from healthy controls.

Few studies have examined BOLD signal variability as a feature in the ML classification of depression, let alone as a feature in any ML algorithm. That being said, Gaut et al. (2019) achieved 84% accuracy using BOLD signal variability to predict the identity of a healthy subject performing a task and the type of task performed within scan sessions. Moreover, they obtained 63% accuracy when assessing the predictive ability of BOLD signal variability for subject identity at rest and found that BOLD signal variability, in general, was reduced during rest in comparison to during tasks.

From these findings, it is evident ML algorithms present a unique opportunity to combine behavioral and functional neuroimaging data in predictive modeling. Furthermore, RF classification appears promising in the classification of MDD diagnosis

and history. That being said, it remains unclear how modeling higher-order measures of neural activity (e.g., BOLD signal variability) would perform and affect the predictive ability of diagnostic classification models in depression.

Aims and Hypotheses

To our knowledge, no studies have yet investigated resting-state BOLD signal variability in relation to varying MDD histories and severities. To that end, evaluating voxel-wise variability as a function of MDD history and severity was a logical next step and could present significant implications for intervention and diagnosis. The current study aimed to determine the alterations in resting-state BOLD signal variability, as measured through the voxel-wise SD of BOLD signal, in both global brain activity and topographical patterns in relation to depression.

Aim 1.

To delineate the differences in voxel-wise resting-state BOLD signal variability between individuals with one of three depression history groups: (*i*) no history of depression; (*ii*) history of depression, but not currently depressed; (*iii*) currently depressed, meeting the diagnostic criteria for a DSM-5 Depressive Disorder.

Hypothesis 1.

The group of individuals with current depression will show less BOLD signal variability in regions of the DMN than individuals with a history of past depression and individuals with no history of depression.

Aim 2.

To determine the relationship between depressive symptom severity and voxel-wise resting-state BOLD signal variability.

Hypothesis 2.

There will be a negative linear relationship between depression symptom severity and average voxel-wise resting-state BOLD signal variability, particularly within regions of the DMN.

Aim 3.

To determine how well the BOLD signal variability in regions of the DMN, SN, and FPN predicts group membership for three depression history groups in comparison to the BOLD signal of those regions.

Hypothesis 3.

BOLD signal variability of regions in DMN, SN, and FPN will have greater feature importance than the BOLD signal of the same regions in classifying individuals into three separate levels of depression history and severity.

Method

Participants

Data were collected for 80 women as a part of a larger NIH R01-funded study investigating the effects of cortisol on cognitive and neural function in depression (Gaffey et al., 2019). All participants were recruited from the Madison, WI area via advertisements sent to counseling centers and clinics as well as paper and digital flyers posted in the community and online. Participants provided written informed consent in accordance with the local IRB and were paid for their participation.

In the larger study, participants completed two fMRI scans typically one week apart (5 - 61 days apart): one placebo scan and one hydrocortisone scan. Hydrocortisone was given to examine alterations in neurocognitive response. An hour prior to each scan,

participants received a pill containing either a placebo or 20 mg hydrocortisone. Drug administration was double-blind and randomized across the two fMRI sessions. Data reported in the current study were taken from the placebo day fMRI scan.

All participants were also screened for psychopathology using the Structured Clinical Interview for the DSM-IV, modified to assess DSM-5 criteria (SCID-I/P for DSM-IV-TR; First, Spitzer, Miriam, & Janet, 2002). Exclusion criteria were as follows: lifetime history of psychosis or mania; current substance use disorder (i.e., within the last 6 months); significant risk for suicide; claustrophobia; daily nicotine use; self-reported use of antidepressants/other psychotropic medications; hormonal contraceptive use; peri- or postmenopausal signs; highly irregular periods; recent pregnancy or breastfeeding (i.e., within the last 6 months); illicit drug use within 4 weeks of participation.

Of the participants with full neuroimaging data available (N = 79), ages ranged from 18 to 45 (M_{age} = 27.6, SD_{age} = 7.0), and they described themselves as White (75%), Asian (16%), and Black (6%). Depending on the level of depression history and severity, participants were categorized into one of three separate groups: (*i*) no history of depression (n = 30; NoDep); (*ii*) history of depression, but not currently depressed (n = 15; PastDep); and (*iii*) currently depressed, meeting the diagnostic criteria for a DSM-5 Depressive Disorder (n = 34; CurrentDep). Participants were also categorized with a 2-level depression history classification: (*i*) no history of depression (n = 30); (*ii*) any history of depression (n = 49; DepHist). With the exception of one subject who received a diagnosis of Social Phobia in partial remission during the SCID interview, participants in the NoDep group did not present with any other psychiatric conditions. Additional participant information can be found in Table 1.

Depression Measure

All participants completed the Beck Depression Inventory-II (BDI-II) at each visit to assess depression severity (Beck et al., 1961). The BDI-II score collected during the placebo day fMRI scan visit was used for all analyses.

fMRI Data Acquisition

All participants were scanned using a 3T GE MRI scanner (Discovery MRI 750; GE Medical Systems, Waukesha, WI) equipped with an 8-channel radiofrequency coil array (GE Healthcare, Waukesha, WI). The resting-state fMRI data were collected using T2*-weighted Echo Planar Imaging (EPI) sequence (TR/TE/FA: 2150 ms/22ms/79°, matrix: 64 x 64, FOV: 22.4 cm, slice thickness: 3.5 mm, voxel size: 3.5 mm x 3.5 mm x 3.5 mm, slices: 40 sagittal) using thin slices and short echo time in order to minimize signal dropout in the ventromedial prefrontal cortex. Each participant was instructed during the resting-state scan (~10 min) to remain "calm, still, and awake" with their eyes open fixating on a cross back-projected onto a screen via an LCD projector (Avotec, Stuart, FL). High-resolution T1-weighted structural imaging data were acquired using a weighted BRAVO pulse sequence (TI: 450ms, TR/TE/flip angle (FA): 8.16 ms/3.2 ms/12°, matrix: 256 x 256 x 160, field of view (FOV): 215.6 mm, slice thickness: 1 mm, voxel size: 1 mm x 1 mm x 1 mm, slices: 156).

Preprocessing and Motion Analysis for rs-fMRI Data

The resting-state fMRI data were preprocessed using AFNI (Cox, 1996) and FSL tools (FMRIB Software Library; http://fsl.fmrib.ox.ac.uk/fsl/fslwiki/). Preprocessing began in AFNI with the calculation of root mean square (RMS) realignment estimates of motion for later inclusion in regression analyses. Preprocessing then continued in FSL

MELODIC with the removal of the first five volumes, interleaved slice-time correction, MCFLIRT motion correction, and spatial smoothing with a 6mm full-width half-maximum (FWHM) Gaussian kernel.

As is common in BOLD signal variability preprocessing (e.g., Nomi et al., 2018), ICA-FIX denoising (Salimi-Khorshidi et al., 2014) was then applied to these data. This began with the hand-classification of components as either noise or signal from 8 randomly selected individuals from each depression group (n = 24) to create a training file of independent component noise features. This training file was then used to regress out common noise components from all participant data. Regression of the Friston 24 motion parameters and linear detrending were additionally applied during ICA-FIX denoising.

Subsequent preprocessing with the noise-cleaned data in AFNI included realignment, co-registration to T1, normalization to MNI space ($3mm^3$), and despiking (3dDespike). Cerebrospinal fluid (CSF), white matter (WM), and gray matter (GM) masks were segmented from normalized T1 anatomical images, and the CSF and WM masks were used in nuisance signal regression. Lastly, the data were bandpass filtered to reflect the low frequency neuronal fluctuations that distinguish resting-state BOLD activity (0.01 – 0.10 Hz).

Statistical Analyses

BOLD signal variability analyses

Calculating BOLD signal variability

BOLD signal variability was calculated for all subjects in AFNI (3dTstat). First, average resting-state BOLD signal was calculated across all voxels for each subject from

the preprocessed time series. Resting-state BOLD signal variability was then calculated as the voxel-wise SD of BOLD signal through subtracting the mean voxel signal from the signal at each time point, squaring this difference, averaging the resulting values across the entire time series, and finally, taking the square root.

$$s = \sqrt{\frac{\sum_{i=1}^{n-1}(x_i - \bar{x}_i)^2}{n-1}}$$

Differences between depression history and BOLD signal variability

To address the current study's first aim of examining differences in BOLD signal variability between individuals with varying depression histories for the entire sample (N = 79), we performed a one-way between-subjects analysis of covariance (ANCOVA) with depression group (NoDep, PastDep, CurrentDep) predicting the voxel-wise resting-state BOLD signal variability in AFNI (3dMVM). As recommended by previous literature, RMS motion estimates were included as a covariate (Martino et al., 2016; Nomi et al., 2017; Nomi et al., 2018). All analyses were family-wise error (FWE) cluster-corrected at the whole-brain level ($p_{FWE} < .05$).

Relation between depression severity and BOLD signal variability

Considering the second aim of this study to investigate the relationship between depressive symptom severity and resting-state BOLD signal variability, a multivariate multiple linear regression analysis was run for the entire sample (N = 79) in AFNI (3dttest++). The model assessed the relationship between resting-state voxel-wise SD of the BOLD signal and the BDI-II score collected on the placebo day fMRI scan visit. RMS motion estimates were also included as a covariate in the regression model. All analyses were FWE cluster-corrected at the whole-brain level ($p_{FWE} < .05$).

Machine learning classification modeling using random forest

All modeling was performed in RStudio 1.2.5033. We utilized a random forest (RF) classification algorithm to address the third aim of the current study. RF modeling was selected for its accuracy, unbiased estimates, ability to balance error in unbalanced datasets, and ability to estimate variable importance (Breiman, 2001; Breiman & Cutler, 2005). For a general overview of the creation of a random forest model, please see Figure 2. Using RF modeling, we aimed to determine how well BOLD signal variability features would predict group membership in comparison to BOLD signal features for three levels of depression history.

We first selected coordinates for 24 ROIs to equally represent the DMN, SN, and FPN (see Table 2; Laird et al., 2009; Seeley et al., 2007). These coordinates were used to create 6-mm radius seed masks in MNI space. Each seed mask was then applied to the fully preprocessed fMRI data of each participant in AFNI (3dfractionize). Next, average BOLD signal and average SD of BOLD signal across all voxels within the mask were calculated (3dROIstats) and extracted to a file compatible with RStudio. Thus, 48 features were collected for the algorithm, including the resting-state BOLD signal and the resting-state BOLD signal variability (24 ROIs x 2 BOLD signal measures = 48 features). Seventy percent of these data were then randomly selected and bootstrapped for a training dataset to create and tune the model, and the remaining 30% of the data were placed in a testing dataset for later model evaluation.

In order to evaluate the model's performance, we applied the RF classifier to the testing dataset and created a confusion matrix to calculate sensitivity, specificity, and accuracy for each level of depression history. From this matrix, we also calculated the

overall accuracy for the model's predictions and created receiver operator characteristic (ROC) curves. To address the specific aim to compare feature importance between BOLD signal features and BOLD signal variability features, we used two measures of variable importance available through the randomForest and caret R packages: mean decrease in accuracy (MDA) and mean decrease in impurity, also known as Gini importance (Gini). Both of these measures look at the unique influence of randomly permuting the values of a single feature on the overall accuracy of predictions. Features with larger positive values for both measures then indicate a variable with greater discriminative power and predictive value.

As is common in machine learning, model optimization was also included to achieve higher rates of classification accuracy. A default model was first established with all standard parameters, including the number of features tried for each decision point of the forest (6) and for the total number of trees in the forest (500). After evaluating the default model's performance, we applied common tuning methods to increase the model's accuracy: increase the total number of trees, increase the number of features at each node, apply a random search to the number of features at each node, apply cross-validation folding techniques to training data (Breiman, 2001; Liaw & Wiener, 2002; Probst, Wright, & Boulesteix, 2019).

Results

Differences between depression histories in BOLD signal variability

Average BOLD signal variability maps were created within each level of depression history (Figure 3) and then entered into the between-groups multivariate ANCOVA in AFNI. Results indicated there were a few regions with different BOLD

signal variability between the three levels of depression history ($p < .001$, uncorrected; Table 3). Additional output from this model further indicated individuals with no history of depression had greater BOLD signal variability than those with current depression in the right cerebellum (Table 3, Figure 4a) and left cerebellum (Table 3, Figure 4b). However, these results did not survive FWE cluster-correction.

Given the largest clusters of BOLD signal variability differences were found between the no history of depression group and the current depression group, we conducted an additional analysis using the 2-level depression history classification. Average BOLD signal variability maps were created within each of the 2 levels of depression history and entered into a multivariate independent samples t-test within AFNI (3dttest++), using depression history (NoDep, DepHist) to predict the average voxel-wise resting-state BOLD signal variability.

There were significant differences in BOLD signal variability in the left and right cerebellum and right lateral parietal cortex between those with no history of depression and individuals with a history of depression ($p_{FWE} < .05$; Table 3, Figure 5). To better visualize the decreased neural signal variability for those with a history of depression, the BOLD signal variability value for the peak voxel of each cluster was extracted and plotted by depression history level (Figure 6).

Relation between depression severity and BOLD signal variability

Depressive symptom severity was negatively related to BOLD signal variability in the cerebellum ($p < .001$, uncorrected; Table 4, Figure 7). In other words, as depression severity increased, the BOLD signal variability within the two cerebellar clusters decreased. However, these results did not survive FWE cluster correction.

Machine learning classification modeling using random forest

Before creating the RF classification algorithm, violin plots were used to visualize the distribution of both BOLD signal and BOLD signal variability features within the three levels of depression history (Figure 8). In classifying observations into one of three levels of depression history, the RF algorithm achieved an overall accuracy of 65.64%. For within class evaluation metrics, including sensitivity, specificity, and accuracy, please refer to Table 5. The corresponding ROC curve reflects the overall accuracy of classification for each depression history level (Figure 9).

The importance of each BOLD signal feature in the overall RF model was plotted using mean decrease in accuracy and Gini importance (Figure 10, Table 6). The top 20 most important variables to model classification according to Gini importance were additionally plotted separately (Figure 11), all of which were BOLD signal variability features. As for the resting-state networks, the DMN (n = 7), SN (n = 7), and FPN (n = 6) were equally represented among the variables with the most discriminative power. Within each network, the most important features were the BOLD signal variability of the left middle temporal gyrus (MTG) in the DMN (*Gini* = 351.16), the BOLD signal variability of the right insula in the SN (*Gini* = 273.91), and the BOLD signal variability of the right inferior temporal gyrus (ITG) of the FPN (*Gini* = 309.33).

In attempts to optimize the RF classifier and mirror the categorical approach used in the first aim, the previous history of depression and current depression groups were combined. First, violin plots were created to visualize the distribution of both BOLD signal and BOLD signal variability features within each level of depression history (Figure 12). An RF classifier was then trained with the *a priori* classifications of “no

history of depression" and "any history of depression". This model achieved 75.79% accuracy distinguishing between the two classes, with 80.82% sensitivity and 74.34% specificity (Table 7). The corresponding ROC curve reflects the overall accuracy (Figure 13). Similar to the 3-level depression history RF classifier, the importance of each BOLD signal feature in the overall RF model was plotted (Figure 14; Table 8), and the top 20 most important variables according to Gini importance were plotted separately (Figure 15). For the top 20 features, 17 were BOLD signal variability features while 3 were average BOLD signal features.

With regard to the resting-state networks, the DMN presented a greater number of important features (n = 10) than the SN (n = 5) and FPN (n = 5). Within each network, the features with the most predictive value were the BOLD signal variability of the left MTG in the DMN (*Gini* = 362.49), the BOLD signal variability of the left frontal pole in the SN (*Gini* = 230.38), and the BOLD signal variability of the right ventrolateral PFC in the FPN (*Gini* = 237.67).

Discussion

To our knowledge, this is the first study to investigate the predictive value of resting-state BOLD signal variability in MDD. More precisely, the present study examined the influence of varying depression history and severity on the standard deviation of resting-state voxel-wise BOLD signal. This study additionally evaluated the importance of resting-state BOLD signal variability measures in predicting depression history through RF classification algorithms.

Partially in line with the first hypothesis, we determined that individuals with a history of depression had significantly decreased resting-state BOLD signal variability

compared to individuals with no history of depression. This difference was localized to three regions: the right cerebellar vermis, the left cerebellar vermis, and a region extending from the right inferior parietal lobule (IPL) to the right superior parietal lobule (SPL). Furthermore, as depressive symptom severity increased, BOLD signal variability within the two cerebellar regions was found to decrease. Although this latter finding was nonsignificant, the locations of the two cerebellar regions were consistent with the initial analyses and reflected the expected direction of the second hypothesis. Thus, the main finding for these two exploratory analyses was that individuals with depression exhibited decreased resting-state BOLD signal variability in the cerebellum and right parietal cortex.

These areas of decreased BOLD signal variability for those with depression are consistent with previous literature investigating alterations in activity and connectivity in depression. For instance, the two clusters found in the left and right vermis of the cerebellum reflect early findings on “cerebellar cognitive affective syndrome” (Schmahmann & Sherman, 1998). This disorder, typically found in individuals with cerebellar degeneration or a lesion, was distinguished by executive dysfunction, language processing deficits, flat affect, and mood swings. In addition, it was found that patients diagnosed with affective disorders presented significantly higher rates of vermal atrophy in comparison to healthy controls (Soares & Mann, 1997). Both studies emphasized the role of the cerebellum’s posterior lobe in mood disorders and subsequently inspired later work using fMRI to investigate the structural and functional differences in the vermis between individuals with depression and healthy controls (Depping et al., 2018a).

In particular, there are 10 vermal lobules in the cerebellum. The current study's findings of decreased BOLD signal variability were localized to lobules VI, VII, and VIII for those with a history of depression. Lobule VII has often shown functional connections with regions of the DMN, while lobules VI and VIII have more often been associated with emotion processing regions (Depping et al., 2018a). Previous work has demonstrated that individuals with depression have significantly decreased rsFC between lobule VII and regions of the DMN, FPN, and reward circuit in comparison to controls (Depping et al., 2018a; Depping, et al., 2018b; Liu et al., 2012a). Likewise, a study using seed-based rsFC with various cerebellar ROIs found significantly reduced connectivity between lobules VI and VIII and the IPL, PFC, and ITG (Guo et al., 2013). The cerebellar dysfunction found in these studies using average BOLD signal measures was later replicated in analyses using neural signal variability measures. For example, Song and colleagues (2017) found significantly lower ALFF and fALFF values in the left cerebellum of an MDD patient group compared to a healthy control group. Comparable changes in fALFF values were also found in the right vermis for individuals with treatment-resistant depression (Yamamura et al., 2016). This evidence of disrupted cerebellar activity is consistent with our findings, suggesting that the activity and function of the vermis may be associated with depression.

BOLD signal variability differences were not limited to the cerebellum, however. The direct comparison of those with no history of depression to those with a history of depression revealed a third region of BOLD signal variability differences in the right lateral parietal cortex. Within this region extending from the right IPL to the SPL, participants with a history of depression exhibited significantly less BOLD signal

variability. In terms of the function of these regions, there has been much work to show the IPL is associated with DMN function, with roles in emotion perception and sensory integration. This region was also recently implicated in the inhibition of mind wandering in healthy subjects through its connections with the PCC (Kajimura et al., 2016). With regard to individuals with depression, the IPL has consistently shown increased activity as well as increased connectivity with other DMN regions (Berman et al., 2011; Greicius et al., 2007; Whitfield-Gabrieli & Ford, 2012; Williams, 2017; Zhu et al., 2012). In contrast, the SPL is more externally oriented, has connections with both FPN and SMN regions, and is involved in visuospatial perception and reasoning, working memory, and attention (Berman et al., 2011; Greicius et al., 2007; Wang et al., 2015; Whitfield-Gabrieli & Ford, 2012; Williams, 2017). This area has shown lower inverse correlations with DMN regions in individuals with depression in comparison to controls (Kaiser et al., 2015; Mulders et al., 2015; Pizzagalli, 2011). Studies using neural signal variability measures have also found functional differences in the right IPL and SPL. Wang et al. (2012) found that MDD patients had significantly lower fALFF values in the right IPL compared to controls. These results were congruent with a later study that reported significantly lower ALFF and fALFF values in the left and right SPL and right IPL for those with depression compared to healthy individuals (Song et al., 2017; Yamamura et al., 2016; Yu et al., 2017).

This previous work in conjunction with the current study's findings clearly indicates that individuals with a history of depression have aberrant neural activity, connectivity, and BOLD signal variability within the posterior cerebellum and right lateral parietal cortex. Moreover, individuals with depression consistently present

decreased brain signal variability within these regions in comparison to healthy individuals. Considering these neurobiological differences in depression history, it was the interest of the final aim to evaluate the predictive value of BOLD signal variability measures in classifying individuals by depression history.

Thus, two RF models were built, with one using a 3-level classification of depression history and a follow-up model using a 2-level classification of depression history. In line with the third hypothesis, the BOLD signal variability features of the DMN, SN, and FPN provided more predictive value in both RF models than the average BOLD signal features of the same regions. For both models, the most important regions for classification within the DMN were the left and right MTG, ventral ACC, precuneus, medial PFC, and the left and right IPL. As for the SN, the left frontal pole and the left and right insula were consistently important. Lastly, the right and left ventrolateral PFC, the right intraparietal sulcus (IPS), and the right ITG were most important in the FPN. Interestingly, there was a greater representation of DMN regions in the 2-level model in comparison to the 3-level model when discriminating between individuals with and without a history of depression.

Although the RF model did not explicitly indicate whether there was greater or reduced BOLD signal variability in these regions for individuals with a history of depression, the locations of these features parallel previous studies using ALFF and fALFF measures. For instance, the most important variable of both models was the BOLD signal variability of the left MTG, an area involved in the DMN and the extended dorsal attention system for its role in attention and working memory. This region has consistently shown decreased fALFF and ALFF values for depressed individuals (Guo et

al., 2012; Wang et al., 2012). With regard to the important regions of the SN, reduced ALFF values within the insula have been reported for increased Hamilton Depression Rating Scale scores in adolescents and young adults with MDD (Liu et al., 2012b). As for the FPN, individuals with depressive symptoms have presented decreased ALFF in the ventrolateral PFC but increased fALFF in the ITG (Wang et al., 2012; Wei et al., 2015). Given these findings, it is probable the regions that were most important for classifying depression history in the RF models have decreased BOLD signal variability for those with a history of depression. This pattern of reduced neural signal variability in depression mirrors both the violin plot visualizations of the BOLD signal variability features (Figures 8 and 12) as well as our earlier findings of decreased BOLD signal variability in the cerebellum and right parietal cortex for individuals with a history of depression.

To summarize, the key finding of the current study is that individuals with a history of depression present decreased neural signal variability in regions important for self-referential thought, emotion processing, and working memory. In other words, there was decreased BOLD signal variability in areas involving externally or internally oriented processing. These findings then highlight a suboptimal level of neural variability that may negatively impact functional network integration. Considering principles from physics and statistics (Burzynska et al., 2015; Easson & McIntosh, 2019; Garrett et al., 2018; Ma et al., 2006), it is known that some amount of variability is required in order for a system to operate normally, and suboptimal levels of variability may affect the entire system. When network integration and temporal variability were directly examined, Garrett et al. (2018) found a robust negative association. The lower the local temporal

variability, the higher the network dimensionality, and the lower the network integration. Similar results were found using functional connectivity, where it was more likely for regional ALFF to positively correlate with the within- and between-network connectivity of the same region (Di et al., 2013). That is to say, the lower the resting-state BOLD signal variability, the lower the rsFC within and between networks.

If we apply these concepts to our findings, one possible interpretation is that the decreased BOLD signal variability found within the cerebellum, DMN, SN, and FPN may be inhibiting normal network communication. As a consequence, the decreased resting-state network integration may contribute to the general neural dysfunction seen in MDD, such as hyperactivity and hyperconnectivity of the DMN (Berman et al., 2011; Whitfield-Gabrieli & Ford, 2012; Zhu et al., 2012). This neural dysfunction then can contribute to greater rumination, persistent thoughts of worthlessness, and negative emotional experience—behaviors that characterize depression. Therefore, BOLD signal variability may contribute to depressive symptoms through its influence on functional network integration. In order to better understand the relation of BOLD signal variability and network integration, future work should investigate the influence of within-network signal variability on both within- and between-network resting-state functional connectivity.

Some limitations are worth noting for this study. First, a few concerns arise from the size of the sample ($N = 79$). Mainly, several recent reviews have discussed the importance of large sample sizes for machine learning classification (Cui & Gong, 2018; Nielsen et al., in press; Zhang et al., 2020). In general, the use of smaller sample sizes may decrease the accuracy and generalizability of machine learning algorithms. Recent

reviews of machine learning classification models advise collecting larger sample sizes of even 10 times the number of features in order to achieve reliable and generalizable accuracy estimates (van der Ploeg et al., 2014). Second, this sample included only female participants. Thus, it is unclear if the differences in BOLD signal variability observed in this study would replicate for males with depression. Future studies could investigate whole-brain, gender-based differences in BOLD signal variability as well as gender-based differences specific to MDD. Third, the methodology for preprocessing resting-state BOLD signal variability and applying voxel-wise corrections are still relatively novel and lack standardization. As recommended by Salimi-Khorshidi and colleagues (2014), noise components for ICA-FIX were hand-labeled by the researchers. Without a standard reference for classifying noise and signal components, it is possible components were incorrectly labeled as noise and regressed from the data. In addition to this, it is unclear how previous recommendations of a strict voxel-wise significance threshold ($p < 0.001$) along with a cluster-wise correction ($p < 0.05$) transfer to resting-state BOLD signal variability analyses. Lastly, differences in BOLD signal variability were examined without accounting for the influence of age. Although a quick analysis of age differences between depression history groups was found to be nonsignificant ($F(2, 76) = 0.14$, $p > 0.05$), previous studies using BOLD signal variability have found age-related functional differences across the lifespan (Garrett et al., 2010; Garrett et al., 2011; Grady & Garrett, 2014; Nomi et al., 2017). It may be important, then, to covary for this demographic measure in future analyses using BOLD signal variability.

Taking into account the high prevalence of MDD (Ferrari et al., 2013; World Health Organization), the current findings may have important implications for clinical

interventions developed to restore optimal neural function in MDD. In particular, repetitive transcranial magnetic stimulation (rTMS) applied to the right parietal cortex and cerebellum appears promising for alleviating depressive symptoms. Compared to individuals given a sham rTMS treatment, individuals given 10 sessions of 2 Hz rTMS to the right parietal cortex presented higher rates of clinical response, defined as 50% or higher reductions in Hamilton Rating Scale for Depression (HAMD) scores (Schutter et al., 2009). Repetitive TMS applied to the medial cerebellum similarly resulted in reduced depressive mood and increased attention in healthy individuals (Schutter et al., 2003; Schutter & van Honk, 2005; van Honk et al., 2003). Aside from treatment implications, our findings also highlight a neurobiological correlate of depression that may underlie other psychiatric conditions with depressive symptoms, such as posttraumatic stress disorder. From this perspective, future research could adopt a transdiagnostic approach and assess the role of neural signal variability in the severity of various psychiatric symptoms.

In conclusion, the current study demonstrates that differences in BOLD signal variability exist between individuals with a history of depression and individuals with no history of depression. The decreased resting-state BOLD signal variability found in the cerebellum and right parietal cortex for those with depression highlights a potential indicator of decreased resting-state network integration and overall neural dysfunction in MDD. More broadly, these findings provide support for this novel approach to investigating aberrant neural activity in depression and provide a better understanding of the resting-state neural correlates of depression.

References

Alexopoulos, G. S., Hoptman, M. J., Kanellopoulos, D., Murphy, C. F., Lim, K. O., & Gunning, F. M. (2012). Functional Connectivity in the Cognitive Control Network and the Default Mode Network in Late-life Depression. *Journal of Affective Disorders*, *139*(1), 56–65.

American Psychiatric Association (2013). *Diagnostic and statistical manual of mental disorders: DSM-5.* Washington, D.C.: American Psychiatric Association.

Beck, A. T., Ward, C. H., Mendelson, M., Mock, J., & Erbaugh, J. (1961). An Inventory for Measuring Depression. *Archives of General Psychiatry*, *4*(6), 561–571.

Beck, J. M., Ma, W. J., Kiani, R., Hanks, T., Churchland, A. K., Roitman, J., Shadlen, M. N., Latham, P. E., & Pouget, A. (2008). Probabilistic population codes for Bayesian decision making. *Neuron*, *60*(6), 1142–1152.

Berman, M. G., Peltier, S., Nee, D. E., Kross, E., Deldin, P. J., & Jonides, J. (2011). Depression, rumination and the default network. *Social Cognitive and Affective Neuroscience*, *6*(5), 548–555.

Breiman, L. (2001). Random Forests. *Machine Learning*, *45*(1), 5–32.

Breiman, L. & Cutler, A. (2005). Random forests. Retrieved from https://www.stat.berkeley.edu/~breiman/RandomForests/cc_home.htm

Burzynska, A. Z., Wong, C. N., Voss, M. W., Cooke, G. E., McAuley, E., & Kramer, A. F. (2015). White matter integrity supports bold signal variability and cognitive performance in the aging human brain. *PLOS ONE*, *10*(4).

Bzdok, D., & Meyer-Lindenberg, A. (2018). Machine Learning for Precision Psychiatry: Opportunities and Challenges. *Biological Psychiatry: Cognitive Neuroscience and Neuroimaging*, *3*(3), 223–230.

Conio, B., Magioncalda, P., Martino, M., Tumati, S., Capobianco, L., Escelsior, A., Adavastro, G., Russo, D., Amore, M., Inglese, M., & Northoff, G. (2019). Opposing patterns of neuronal variability in the sensorimotor network mediate cyclothymic and depressive temperaments. *Human Brain Mapping*, *40*(4), 1344–1352

Cox, R. W. (1996). AFNI: Software for analysis and visualization of functional magnetic resonance neuroimages. *Computers and Biomedical Research, an International Journal*, *29*(3), 162–173.

Cui, Z., & Gong, G. (2018). The effect of machine learning regression algorithms and sample size on individualized behavioral prediction with functional connectivity features. *NeuroImage*, *178*, 622–637.

Damoiseaux, J. S., & Greicius, M. D. (2009). Greater than the sum of its parts: A review of studies combining structural connectivity and resting-state functional connectivity. *Brain Structure & Function*, *213*(6), 525–533.

Depping, M. S., Schmitgen, M. M., Kubera, K. M., & Wolf, R. C. (2018a). Cerebellar Contributions to Major Depression. *Frontiers in Psychiatry*, *9*, 634.

Depping, M. S., Wolf, N. D., Vasic, N., Sosic-Vasic, Z., Schmitgen, M. M., Sambataro, F., & Wolf, R. C. (2018b). Aberrant resting-state cerebellar blood flow in major depression. *Journal of Affective Disorders*, *226*, 227–231.

Di, X., Kim, E. H., Huang, C.-C., Lin, C.-P., & Biswal, B. (2013). The Influence of the Amplitude of Low-Frequency Fluctuations on Resting-State Functional Connectivity. *Frontiers in Human Neuroscience*, *7*, 118.

Drevets, W. C., Price, J. L., & Furey, M. L. (2008). Brain structural and functional abnormalities in mood disorders: Implications for neurocircuitry models of depression. *Brain Structure & Function*, *213*(1–2), 93–118.

Easson, A. K., & McIntosh, A. R. (2019). BOLD signal variability and complexity in children and adolescents with and without autism spectrum disorder. *Developmental Cognitive Neuroscience*, *36*, 100630.

Ferrari, A. J., Charlson, F. J., Norman, R. E., Patten, S. B., Freedman, G., Murray, C. J. L., Vos, T., & Whiteford, H. A. (2013). Burden of Depressive Disorders by Country, Sex, Age, and Year: Findings from the Global Burden of Disease Study 2010. *PLOS Medicine*, *10*(11), e1001547.

First, M. B., Spitzer, R. L., Miriam, G., & Janet, B. W. (2002). *Structured Clinical Interview for DSM-IV-TR Axis I Disorders*, Research Version, Patient Edition. New York: Biometrics Research, New York State Psychiatric Institute.

Folstein, M. F., Robinson, R., Folstein, S., & McHugh, P. R. (1985). Depression and neurological disorders: New treatment opportunities for elderly depressed patients. *Journal of Affective Disorders*, *8*, S11–S14.

Gaffey, A. E., Walsh, E. C., Ladd, C. O., Hoks, R. M., & Abercrombie, H. C. (2019). Alterations in Systemic and Cognitive Glucocorticoid Sensitivity in Depression. *Biological Psychiatry: Cognitive Neuroscience and Neuroimaging*, *4*(3), 310–320.

Garrett, D. D., Epp, S. M., Perry, A., & Lindenberger, U. (2018). Local temporal variability reflects functional integration in the human brain. *NeuroImage*, *183*, 776–787.

Garrett, D. D., Kovacevic, N., McIntosh, A. R., & Grady, C. L. (2010). Blood oxygen level-dependent signal variability is more than just noise. *Journal of Neuroscience*, *30*(14), 4914–4921.

Garrett, D. D., Kovacevic, N., McIntosh, A. R., & Grady, C. L. (2011). The importance of being variable. *Journal of Neuroscience*, *31*(12), 4496–4503.

Gaut, G., Turner, B., Lu, Z.-L., Li, X., Cunningham, W. A., & Steyvers, M. (2019). Predicting task and subject differences with functional connectivity and blood-oxygen-level-dependent variability. *Brain Connectivity*, *9*(6), 451–463.

Gosnell, S. N., Fowler, J. C., & Salas, R. (2019). Classifying suicidal behavior with resting-state functional connectivity and structural neuroimaging. *Acta Psychiatrica Scandinavica*, *140*(1), 20–29.

Grady, C. L., & Garrett, D. D. (2014). Understanding variability in the BOLD signal and why it matters for aging. *Brain Imaging and Behavior*, *8*(2), 274–283.

Greicius, M. D., Flores, B. H., Menon, V., Glover, G. H., Solvason, H. B., Kenna, H., Reiss, A. L., & Schatzberg, A. F. (2007). Resting-state functional connectivity in major depression: Abnormally increased contributions from subgenual cingulate cortex and thalamus. *Biological Psychiatry*, *62*(5), 429–437.

Guo, C. C., Nguyen, V. T., Hyett, M. P., Parker, G. B., & Breakspear, M. J. (2015). Out-of-sync: Disrupted neural activity in emotional circuitry during film viewing in melancholic depression. *Scientific Reports*, *5*, 11605.

Guo, W., Liu, F., Xue, Z., Gao, K., Liu, Z., Xiao, C., Chen, H., & Zhao, J. (2013). Abnormal resting-state cerebellar–cerebral functional connectivity in treatment-resistant depression and treatment sensitive depression. *Progress in Neuro-Psychopharmacology and Biological Psychiatry*, *44*, 51–57.

Guo, W., Liu, F., Xue, Z., Xu, X., Wu, R., Ma, C., Wooderson, S. C., Tan, C., Sun, X., Chen, J., Liu, Z., Xiao, C., Chen, H., & Zhao, J. (2012). Alterations of the amplitude of low-frequency fluctuations in treatment-resistant and treatment-response depression: A resting-state fMRI study. *Progress in Neuro-Psychopharmacology and Biological Psychiatry*, *37*(1), 153–160.

Haslam, N., & Beck, A. T. (1993). Categorization of major depression in an outpatient sample. *Journal of Nervous and Mental Disease*, *181*(12), 725–731.

Jahedi, A., Nasamran, C. A., Faires, B., Fan, J., & Müller, R.-A. (2017). Distributed Intrinsic Functional Connectivity Patterns Predict Diagnostic Status in Large Autism Cohort. *Brain Connectivity*, *7*(8), 515–525.

Kaiser, R. H., Andrews-Hanna, J. R., Wager, T. D., & Pizzagalli, D. A. (2015). Large-Scale Network Dysfunction in Major Depressive Disorder: A Meta-analysis of Resting-State Functional Connectivity. *JAMA Psychiatry*, *72*(6), 603–611.

Kajimura, S., Kochiyama, T., Nakai, R., Abe, N., & Nomura, M. (2016). Causal relationship between effective connectivity within the default mode network and mind-wandering regulation and facilitation. *NeuroImage*, *133*, 21–30.

Kebets, V., Houenou, J., Küng, A.-L., Hamdani, N., Leboyer, M., Aubry, J.-M., Dayer, A., Van de Ville, D., & Piguet, C. (2018). S133. Resting state bold signal

variability correlates with clinical dimensions in euthymic bipolar patients. *Biological Psychiatry*, *83*(9, Supplement), S399.

Laird, A. R., Eickhoff, S. B., Li, K., Robin, D. A., Glahn, D. C., & Fox, P. T. (2009). Investigating the functional heterogeneity of the default mode network using coordinate-based meta-analytic modeling. *The Journal of Neuroscience*, *29*(46), 14496–14505.

Li, L., Wang, Y., Ye, L., Chen, W., Huang, X., Cui, Q., He, Z., Liu, D., & Chen, H. (2019). Altered brain signal variability in patients with generalized anxiety disorder. *Frontiers in Psychiatry*, *10*.

Liaw, A. & Wiener, M. (2002). Classification and regression by randomForest. *R News, 2/3*, 18-22.

Liston, C., Chen, A. C., Zebley, B. D., Drysdale, A. T., Gordon, R., Leuchter, B., Voss, H. U., Casey, B. J., Etkin, A., & Dubin, M. J. (2014). Default Mode Network Mechanisms of Transcranial Magnetic Stimulation in Depression. *Biological Psychiatry*, *76*(7), 517–526.

Liu, C.-H., Li, F., Li, S.-F., Wang, Y.-J., Tie, C.-L., Wu, H.-Y., Zhou, Z., Zhang, D., Dong, J., Yang, Z., & Wang, C.-Y. (2012b). Abnormal baseline brain activity in bipolar depression: A resting state functional magnetic resonance imaging study. *Psychiatry Research: Neuroimaging*, *203*(2), 175–179.

Liu, L., Zeng, L.-L., Li, Y., Ma, Q., Li, B., Shen, H., & Hu, D. (2012a). Altered cerebellar functional connectivity with intrinsic connectivity networks in adults with major depressive disorder. *PLOS ONE*, *7*(6), e39516–e39516. PubMed.

Ma, W. J., Beck, J. M., Latham, P. E., & Pouget, A. (2006). Bayesian inference with probabilistic population codes. *Nature Neuroscience*, *9*(11), 1432–1438.

Manoliu, A., Meng, C., Brandl, F., Doll, A., Tahmasian, M., Scherr, M., Schwerthöffer, D., Zimmer, C., Förstl, H., Bäuml, J., Riedl, V., Wohlschläger, A., & Sorg, C. (2014). Insular dysfunction within the salience network is associated with severity of symptoms and aberrant inter-network connectivity in major depressive disorder. *Frontiers in Human Neuroscience*, *7*.

Månsson, K., Garrett, D., Manzouri, A., Wiegert, S., Furmark, T., & Fischer, H. (2018). F31. Affective brain signal variability separates social anxiety disorder patients from healthy individuals. *Biological Psychiatry*, *83*(9, Supplement), S249–S250.

Martino, M., Magioncalda, P., Huang, Z., Conio, B., Piaggio, N., Duncan, N. W., Rocchi, G., Escelsior, A., Marozzi, V., Wolff, A., Inglese, M., Amore, M., & Northoff, G. (2016). Contrasting variability patterns in the default mode and sensorimotor networks balance in bipolar depression and mania. *Proceedings of the National Academy of Sciences*, *113*(17), 4824–4829.

Mulders, P. C., van Eijndhoven, P. F., Schene, A. H., Beckmann, C. F., & Tendolkar, I. (2015). Resting-state functional connectivity in major depressive disorder: A review. *Neuroscience and Biobehavioral Reviews*, *56*, 330–344.

Mumtaz, W., Ali, S. S. A., Yasin, M. A. M., & Malik, A. S. (2018). A machine learning framework involving EEG-based functional connectivity to diagnose major depressive disorder (MDD). *Medical & Biological Engineering & Computing*, *56*(2), 233–246.

Nielsen, A. N., Barch, D. M., Petersen, S. E., Schlaggar, B. L., & Greene, D. J. (In Press). Machine Learning With Neuroimaging: Evaluating Its Applications in Psychiatry. *Biological Psychiatry: Cognitive Neuroscience and Neuroimaging*.

Nomi, J. S., Bolt, T. S., Ezie, C. E. C., Uddin, L. Q., & Heller, A. S. (2017). Moment-to-moment bold signal variability reflects regional changes in neural flexibility across the lifespan. *The Journal of Neuroscience*, *37*(22), 5539–5548.

Nomi, J. S., Schettini, E., Voorhies, W., Bolt, T. S., Heller, A. S., & Uddin, L. Q. (2018). Resting-state brain signal variability in prefrontal cortex is associated with ADHD symptom severity in children. *Frontiers in Human Neuroscience*, *12*.

Ongür, D., Ferry, A. T., & Price, J. L. (2003). Architectonic subdivision of the human orbital and medial prefrontal cortex. *The Journal of Comparative Neurology*, *460*(3), 425–449.

Patel, M. J., Andreescu, C., Price, J. C., Edelman, K. L., Reynolds, C. F., & Aizenstein, H. J. (2015). Machine learning approaches for integrating clinical and imaging features in late-life depression classification and response prediction. *International Journal of Geriatric Psychiatry*, *30*(10), 1056–1067.

Patel, M. J., Khalaf, A., & Aizenstein, H. J. (2016). Studying depression using imaging and machine learning methods. *NeuroImage: Clinical*, *10*, 115–123.

Perugi, G., Toni, C., Maremmani, I., Tusini, G., Ramacciotti, S., Madia, A., Fornaro, M., & Akiskal, H. S. (2012). The influence of affective temperaments and psychopathological traits on the definition of bipolar disorder subtypes: A study on bipolar I Italian national sample. *Journal of Affective Disorders*, *136*(1–2), e41–e49.

Phillips, M. L., Drevets, W. C., Rauch, S. L., & Lane, R. (2003). Neurobiology of emotion perception II: Implications for major psychiatric disorders. *Biological Psychiatry*, *54*(5), 515–528.

Pizzagalli, D. A. (2011). Frontocingulate dysfunction in depression: Toward biomarkers of treatment response. *Neuropsychopharmacology: Official Publication of the American College of Neuropsychopharmacology*, *36*(1), 183–206.

Probst, P., Wright, M., & Boulesteix, A.-L. (2019). Hyperparameters and tuning strategies for random forest. *Wiley Interdisciplinary Reviews: Data Mining and Knowledge Discovery*, *9*(3).

Ramasubbu, R., Konduru, N., Cortese, F., Bray, S., Gaxiola-Valdez, I., & Goodyear, B. (2014). Reduced Intrinsic Connectivity of Amygdala in Adults with Major Depressive Disorder. *Frontiers in Psychiatry*, *5*.

Rutledge, R. B., Chekroud, A. M., & Huys, Q. J. (2019). Machine learning and big data in psychiatry: Toward clinical applications. *Current Opinion in Neurobiology*, *55*, 152–159.

Sacchet, M. D., Prasad, G., Foland-Ross, L. C., Thompson, P. M., & Gotlib, I. H. (2015). Support Vector Machine Classification of Major Depressive Disorder Using Diffusion-Weighted Neuroimaging and Graph Theory. *Frontiers in Psychiatry*, *6*.

Salimi-Khorshidi, G., Douaud, G., Beckmann, C. F., Glasser, M. F., Griffanti, L., & Smith, S. M. (2014). Automatic denoising of functional MRI data: Combining independent component analysis and hierarchical fusion of classifiers. *NeuroImage*, *90*, 449–468.

Scarapicchia, V., Mazerolle, E. L., Fisk, J. D., Ritchie, L. J., & Gawryluk, J. R. (2018). Resting state BOLD variability in Alzheimer's Disease: A marker of cognitive decline or cerebrovascular status? *Frontiers in Aging Neuroscience*, *10*.

Schmahmann, J. D., & Sherman, J. C. (1998). The cerebellar cognitive affective syndrome. *Brain*, *121*(4), 561–579.

Schutter, D. J. L. G., Martin Laman, D., van Honk, J., Vergouwen, A. C., & Frank Koerselman, G. (2009). Partial clinical response to 2 weeks of 2 Hz repetitive transcranial magnetic stimulation to the right parietal cortex in depression. *International Journal of Neuropsychopharmacology*, *12*(5), 643–650.

Schutter, D. J. L. G., & van Honk, J. (2005). A framework for targeting alternative brain regions with repetitive transcranial magnetic stimulation in the treatment of depression. *Journal of Psychiatry & Neuroscience : JPN*, *30*(2), 91–97. PubMed.

Schutter, D. J. L. G., van Honk, J., d'Alfonso, A. A. L., Peper, J. S., & Panksepp, J. (2003). High frequency repetitive transcranial magnetic over the medial cerebellum induces a shift in the prefrontal electroencephalography gamma spectrum: A pilot study in humans. *Neuroscience Letters*, *336*(2), 73–76.

Seeley, W. W., Menon, V., Schatzberg, A. F., Keller, J., Glover, G. H., Kenna, H., Reiss, A. L., & Greicius, M. D. (2007). Dissociable intrinsic connectivity networks for salience processing and executive control. *The Journal of Neuroscience: The Official Journal of the Society for Neuroscience*, *27*(9), 2349–2356.

Sheline, Y. I., Barch, D. M., Price, J. L., Rundle, M. M., Vaishnavi, S. N., Snyder, A. Z., Mintun, M. A., Wang, S., Coalson, R. S., & Raichle, M. E. (2009). The default

mode network and self-referential processes in depression. *Proceedings of the National Academy of Sciences*, *106*(6), 1942–1947.

Shimizu, Y., Yoshimoto, J., Toki, S., Takamura, M., Yoshimura, S., Okamoto, Y., Yamawaki, S., & Doya, K. (2015). Toward probabilistic diagnosis and understanding of depression based on functional MRI data analysis with logistic group LASSO. *PLOS ONE*, *10*(5), e0123524.

Soares, J. C., & Mann, J. J. (1997). The anatomy of mood disorders—Review of structural neuroimaging studies. *Biological Psychiatry*, *41*(1), 86–106.

Song, Y., Sun, S., Song, X., Mao, N., & Wang, B. (2017). BOLD-fMRI study on the basic activity of the brain in major disorder depression and their first-degree relatives. *Journal of Practical Radiology*, *33*(5), 653–657.

Tahmasian, M., Knight, D. C., Manoliu, A., Schwerthöffer, D., Scherr, M., Meng, C., Shao, J., Peters, H., Doll, A., Khazaie, H., Drzezga, A., Bäuml, J., Zimmer, C., Förstl, H., Wohlschläger, A. M., Riedl, V., & Sorg, C. (2013). Aberrant Intrinsic Connectivity of Hippocampus and Amygdala Overlap in the Fronto-Insular and Dorsomedial-Prefrontal Cortex in Major Depressive Disorder. *Frontiers in Human Neuroscience*, *7*.

van den Heuvel, M. P., & Hulshoff Pol, H. E. (2010). Exploring the brain network: A review on resting-state fMRI functional connectivity. *European Neuropsychopharmacology: The Journal of the European College of Neuropsychopharmacology*, *20*(8), 519–534.

van der Ploeg, T., Austin, P. C., & Steyerberg, E. W. (2014). Modern modelling techniques are data hungry: A simulation study for predicting dichotomous endpoints. *BMC Medical Research Methodology*, *14*(1), 137.

van Honk, J., Schutter, D. J. L. G., Putman, P., de Haan, E. H. F., & d'Alfonso, A. A. L. (2003). Reductions in phenomenological, physiological and attentional indices of depressive mood after 2 Hz rTMS over the right parietal cortex in healthy human subjects. *Psychiatry Research*, *120*(1), 95–101.

Wade, B. S. C., Joshi, S. H., Pirnia, T., Leaver, A. M., Woods, R. P., Thompson, P. M., Espinoza, R., & Narr, K. L. (2015). Random forest classification of depression status based on subcortical brain morphometry following electroconvulsive therapy. *2015 IEEE 12th International Symposium on Biomedical Imaging, ISBI 2015*, 92–96.

Wang, J., Yang, Y., Fan, L., Xu, J., Li, C., Liu, Y., Fox, P. T., Eickhoff, S. B., Yu, C., & Jiang, T. (2015). Convergent functional architecture of the superior parietal lobule unraveled with multimodal neuroimaging approaches. *Human Brain Mapping*, *36*(1), 238–257. PubMed.

Wang, L., Dai, W., Su, Y., Wang, G., Tan, Y., Jin, Z., Zeng, Y., Yu, X., Chen, W., Wang, X., & Si, T. (2012). Amplitude of low-frequency oscillations in first-episode, treatment-naive patients with major depressive disorder: A resting-state functional MRI study. *PLOS ONE*, *7*(10), e48658–e48658. PubMed.

Wei, X., Shen, H., Ren, J., Liu, W., Yang, R., Liu, J., Wu, H., Xu, X., Lai, L., Hu, J., Pan, X., & Jiang, X. (2015). Alteration of spontaneous neuronal activity in young

adults with non-clinical depressive symptoms. *Psychiatry Research: Neuroimaging*, *233*(1), 36–42.

Whitfield-Gabrieli, S., & Ford, J. M. (2012). Default mode network activity and connectivity in psychopathology. *Annual Review of Clinical Psychology*, *8*(1), 49–76.

Williams, L. M. (2017). Defining biotypes for depression and anxiety based on large-scale circuit dysfunction: A theoretical review of the evidence and future directions for clinical translation. *Depression and Anxiety*, *34*(1), 9–24.

World Health Organization. Depression and other common mental disorders: global health estimates. Geneva: World Health Organization, 2017.

Yamamura, T., Okamoto, Y., Okada, G., Takaishi, Y., Takamura, M., Mantani, A., Kurata, A., Otagaki, Y., Yamashita, H., & Yamawaki, S. (2016). Association of thalamic hyperactivity with treatment-resistant depression and poor response in early treatment for major depression: A resting-state fMRI study using fractional amplitude of low-frequency fluctuations. *Translational Psychiatry*, *6*(3), e754–e754.

Yu, H.-L., Liu, W.-B., Wang, T., Huang, P., Jie, L.-Y., Sun, J.-Z., Wang, C., Qian, W., Xuan, M., & Gu, Q.-Q. (2017). Difference in resting-state fractional amplitude of low-frequency fluctuation between bipolar depression and unipolar depression patients. *European Review for Medical and Pharmacological Sciences*, *21*, 1541–1550.

Zeng, L.-L., Shen, H., Liu, L., & Hu, D. (2014). Unsupervised classification of major depression using functional connectivity MRI. *Human Brain Mapping*, *35*(4), 1630–1641.

Zeng, L.-L., Shen, H., Liu, L., Wang, L., Li, B., Fang, P., Zhou, Z., Li, Y., & Hu, D. (2012). Identifying major depression using whole-brain functional connectivity: A multivariate pattern analysis. *Brain*, *135*(5), 1498–1507.

Zhang, J., Cheng, W., Liu, Z., Zhang, K., Lei, X., Yao, Y., Becker, B., Liu, Y., Kendrick, K. M., Lu, G., & Feng, J. (2016). Neural, electrophysiological and anatomical basis of brain-network variability and its characteristic changes in mental disorders. *Brain*, *139*(8), 2307–2321.

Zhang, X., Braun, U., Tost, H., & Bassett, D. S. (2020). Data-Driven Approaches to Neuroimaging Analysis to Enhance Psychiatric Diagnosis and Therapy. *Biological Psychiatry: Cognitive Neuroscience and Neuroimaging*.

Zhu, X., Wang, X., Xiao, J., Liao, J., Zhong, M., Wang, W., & Yao, S. (2012). Evidence of a dissociation pattern in resting-state default mode network connectivity in first-episode, treatment-naive major depression patients. *Biological Psychiatry*, *71*(7), 611–617.

Figures

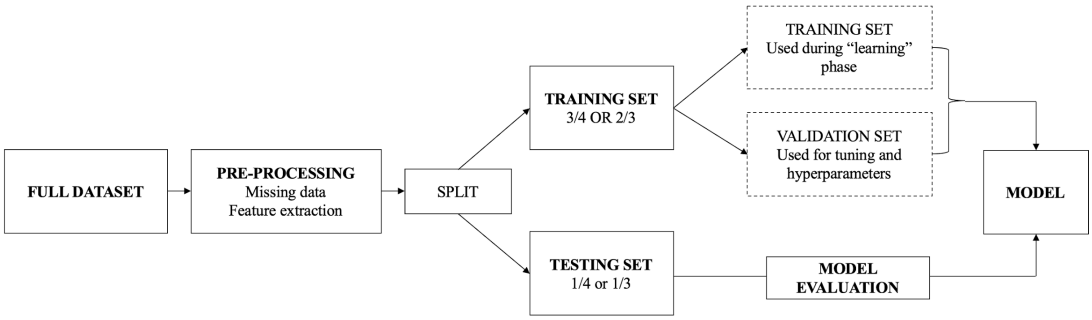

Figure 1. Approach to building supervised classification machine learning algorithm.

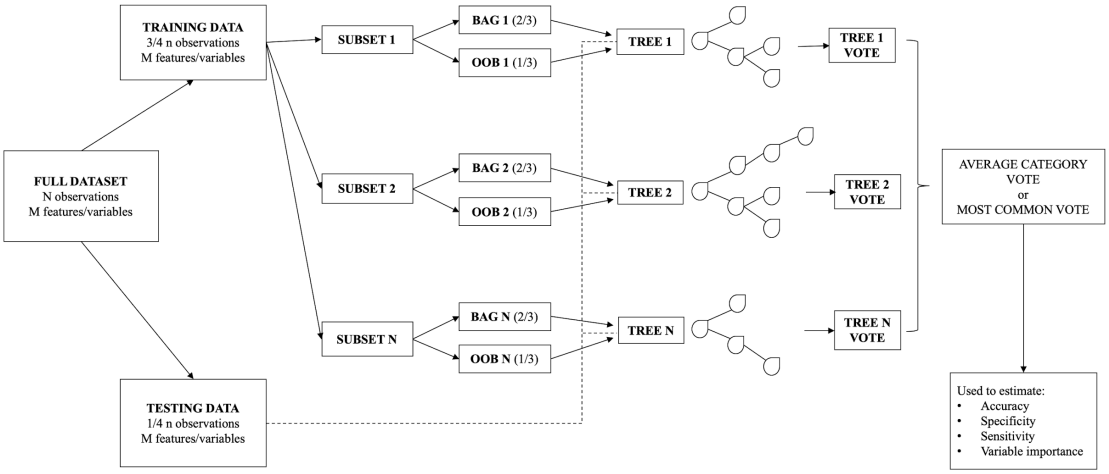

Figure 2. Graphic representation of creating and testing a random forest algorithm. Note "BAG" refers to randomly selected subset and bootstrapped observations and features, while "OOB" refers to withheld, randomly selected subset and bootstrapped observations and features.

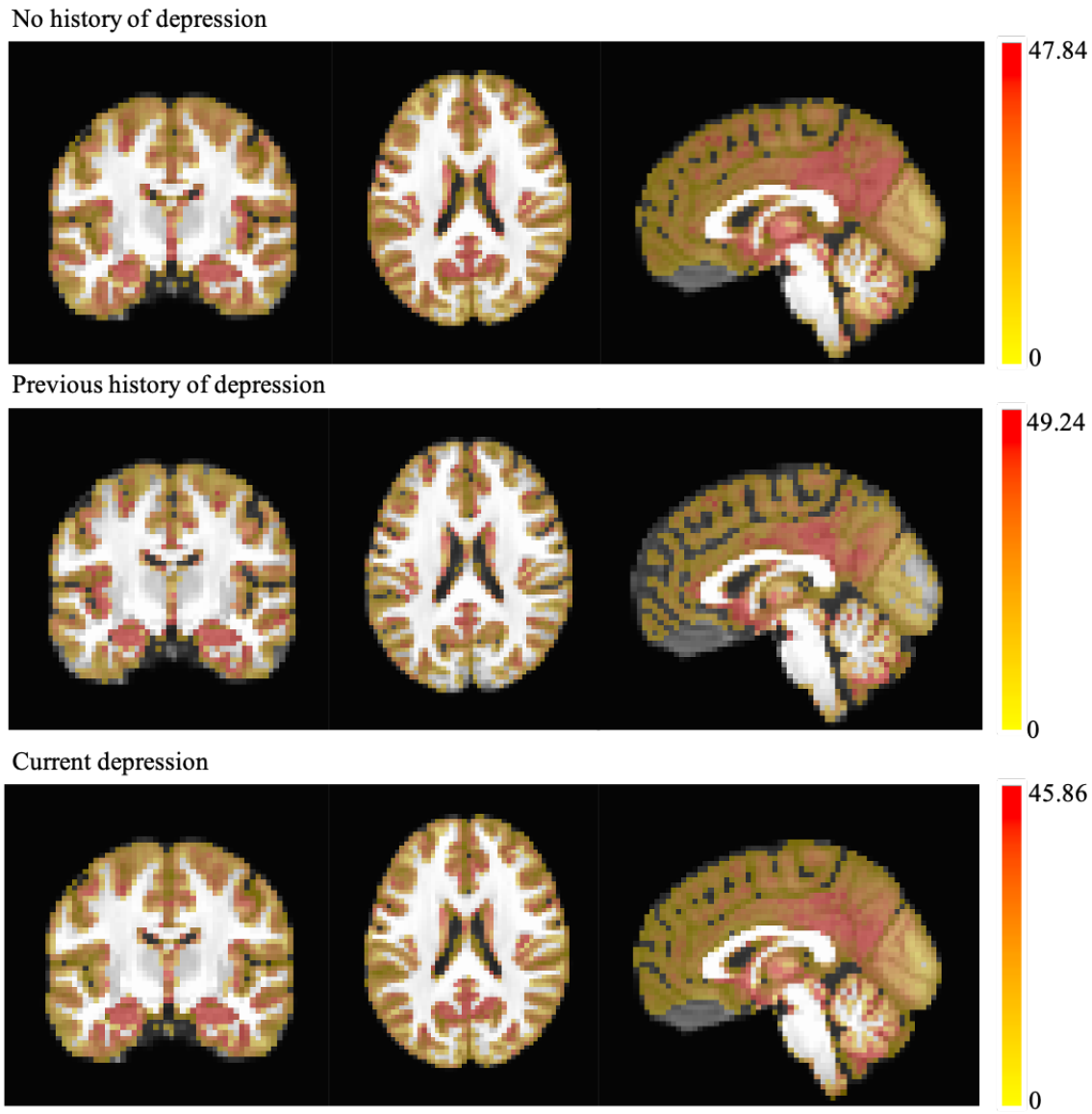

Figure 3. Average BOLD signal variability maps within the three levels of depression history. Greater BOLD signal variability depicted in red regions and less BOLD signal variability in yellow regions.

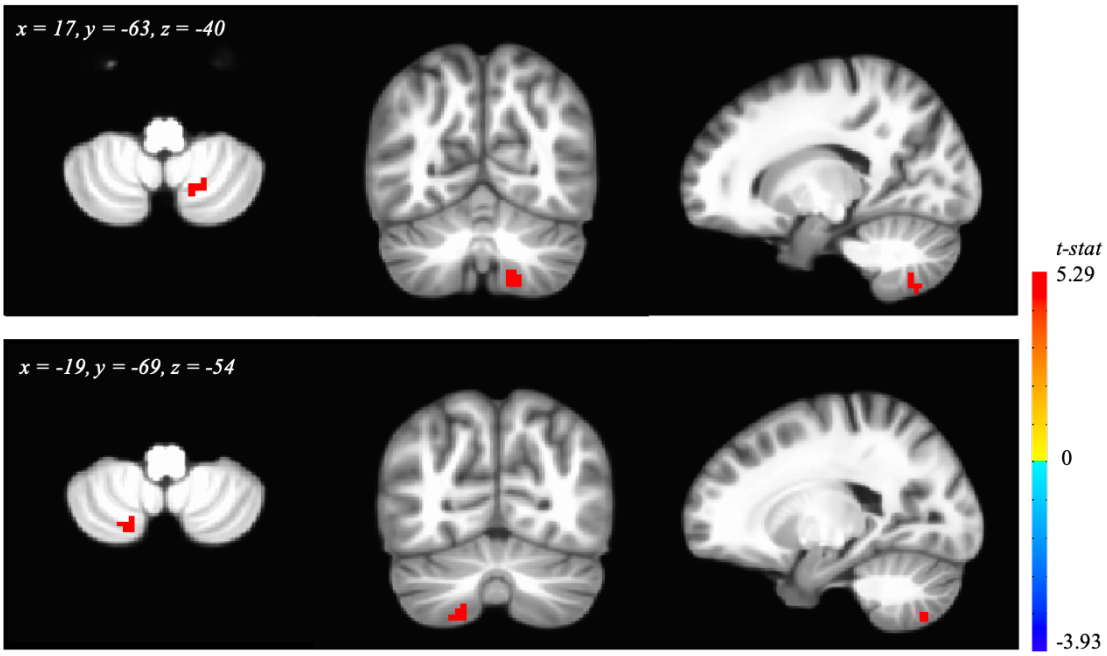

Figure 4. *Post-hoc* results from the Aim 1 multivariate between-groups ANCOVA using depression history group to predict resting-state voxel-wise BOLD signal variability. Depicted are the two largest clusters showing differences in BOLD signal variability between those with no history of depression and those with current depression ($p < .001$, uncorrected).

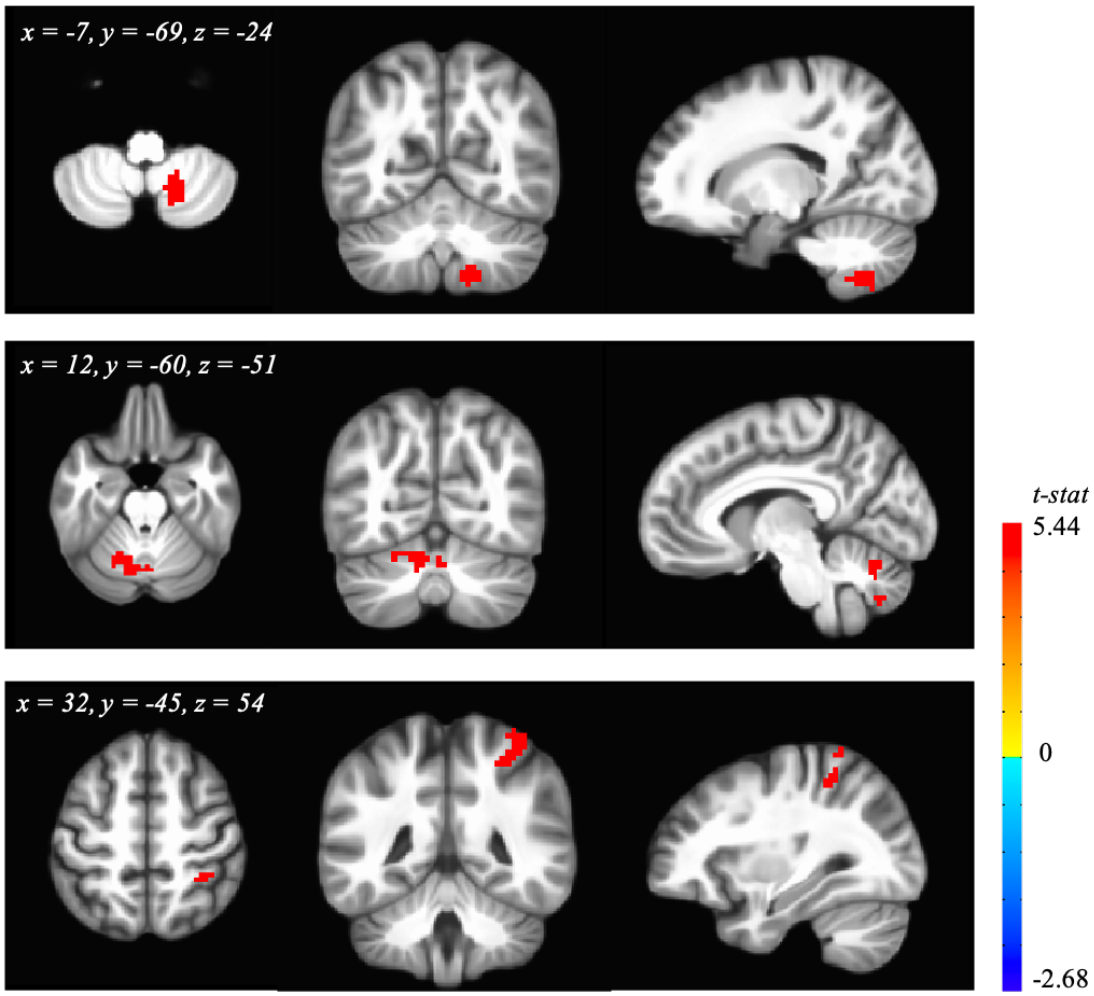

Figure 5. Results from the follow-up, multivariate two sample t-test comparison of resting-state voxel-wise BOLD signal variability between individuals with no history of depression and individuals with any history of depression ($p_{FWE} < .05$).

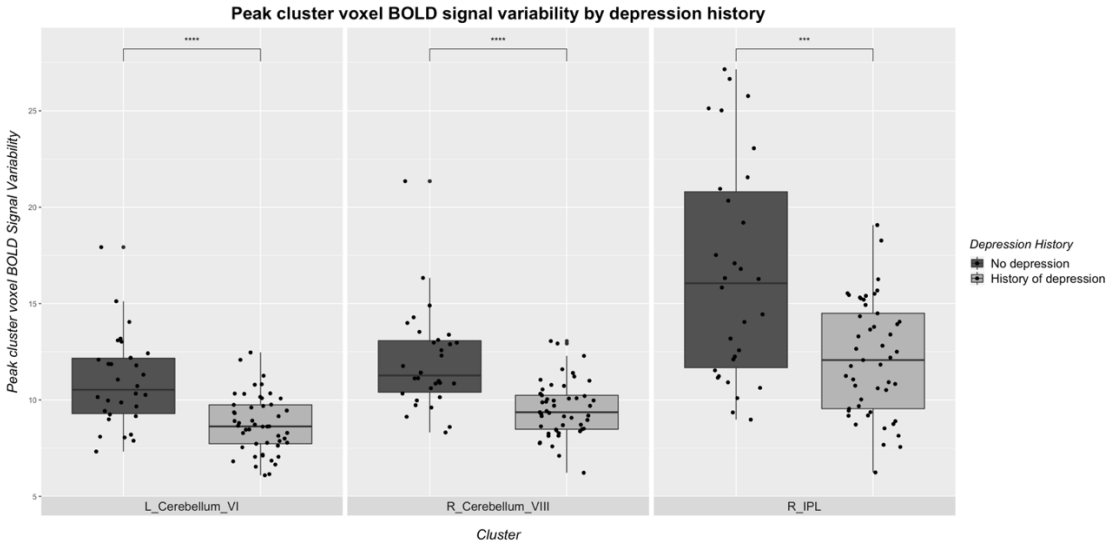

Figure 6. BOLD signal variability at the peak voxel of each significant cluster found in the follow-up, multivariate two sample *t*-test comparison between individuals with no history of depression (represented in dark gray) and individuals with any history of depression (represented in light gray).

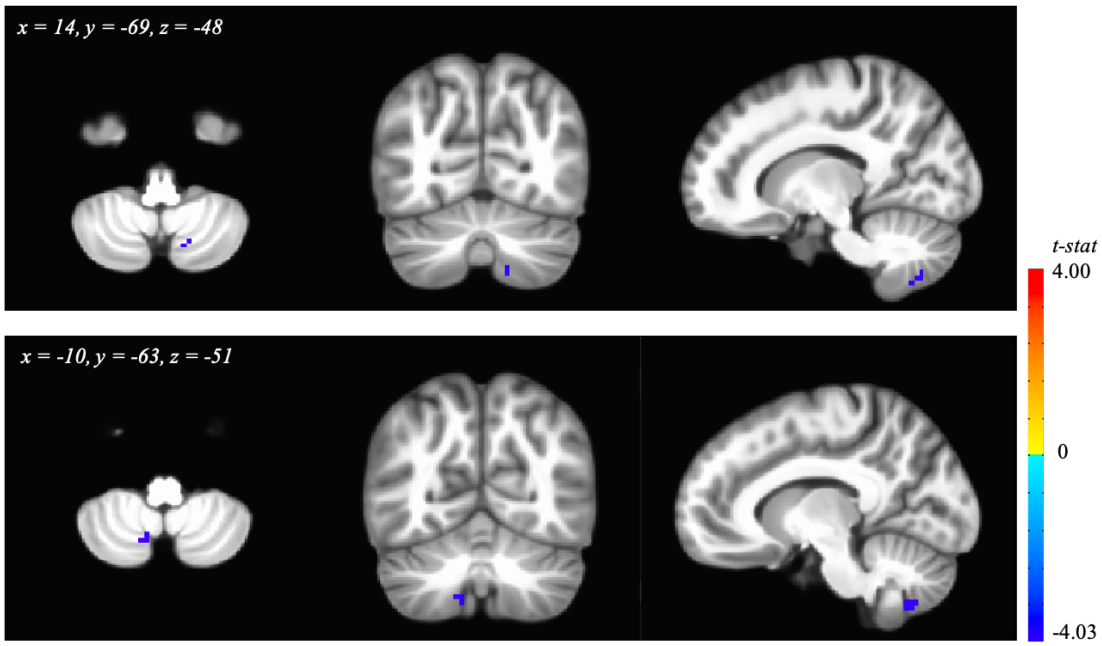

Figure 7. Results from the Aim 2 multivariate multiple linear regression looking at the relationship of resting-state voxel-wise BOLD signal variability and depressive symptom severity ($p < .001$, uncorrected).

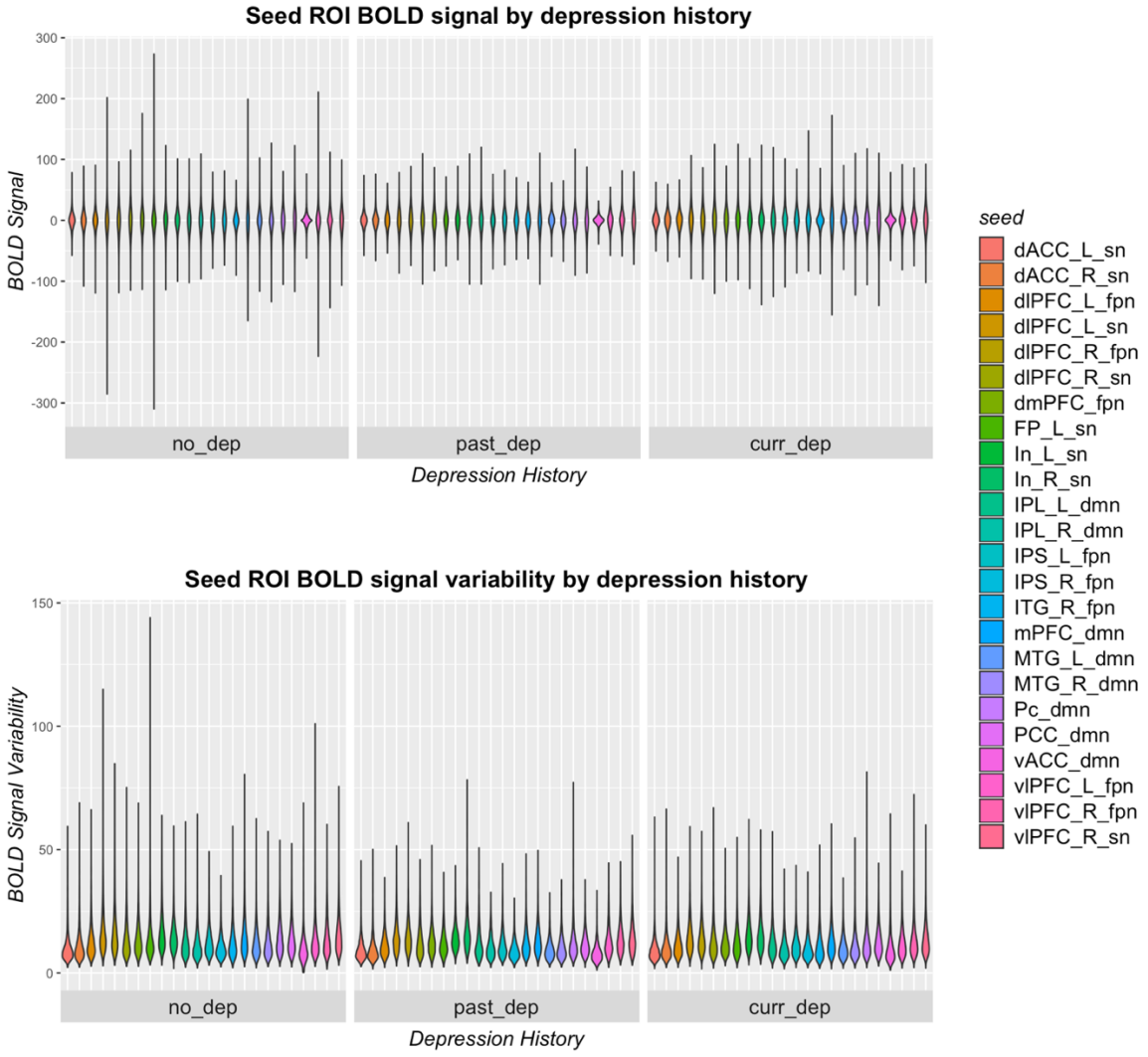

Figure 8. Violin plots illustrating the distribution of BOLD signal features (*top*) and BOLD signal variability features (*bottom*) within three levels of depression history.

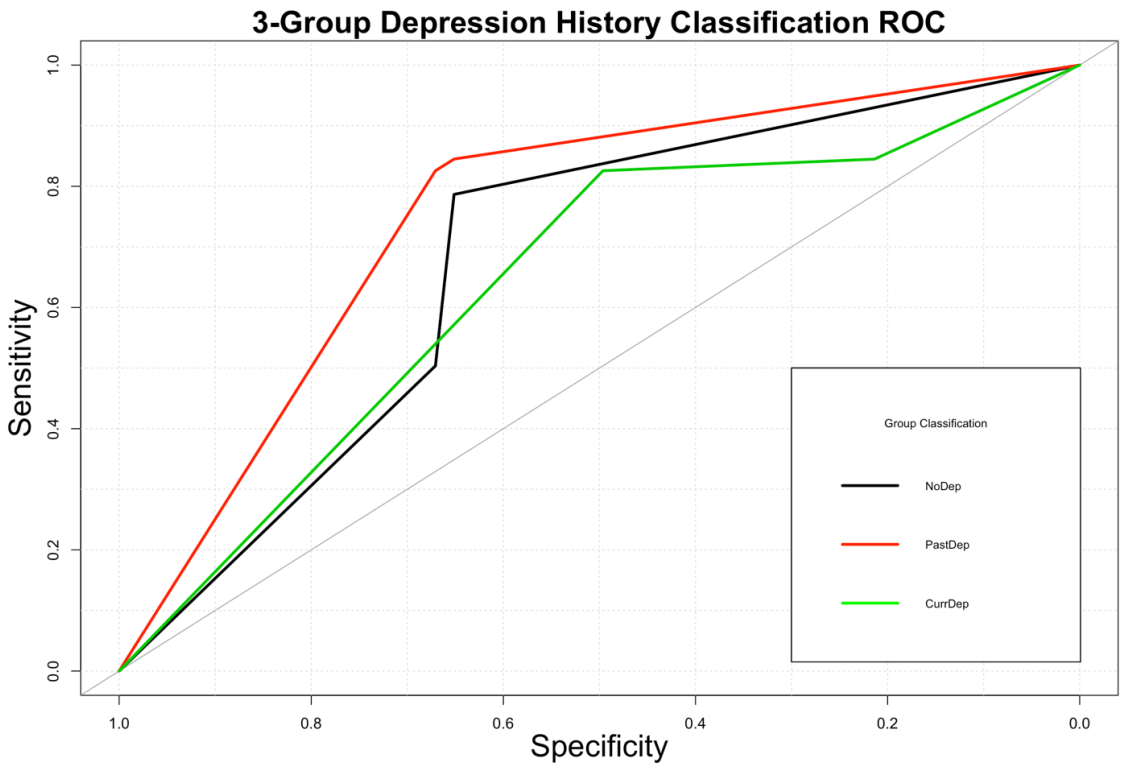

Figure 9. ROC curve for the 3-level depression history classification random forest.

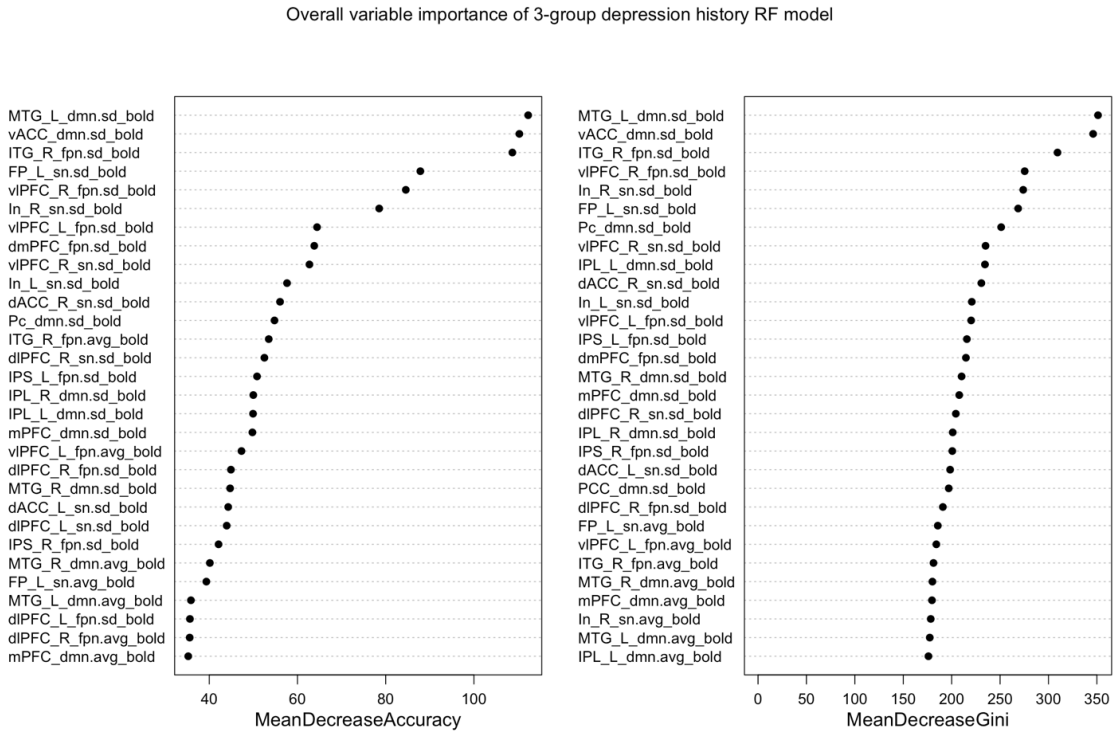

Figure 10. Variable importance plot including mean decrease in accuracy and Gini importance for the 3-level depression history classification random forest (randomForest::varImpPlot).

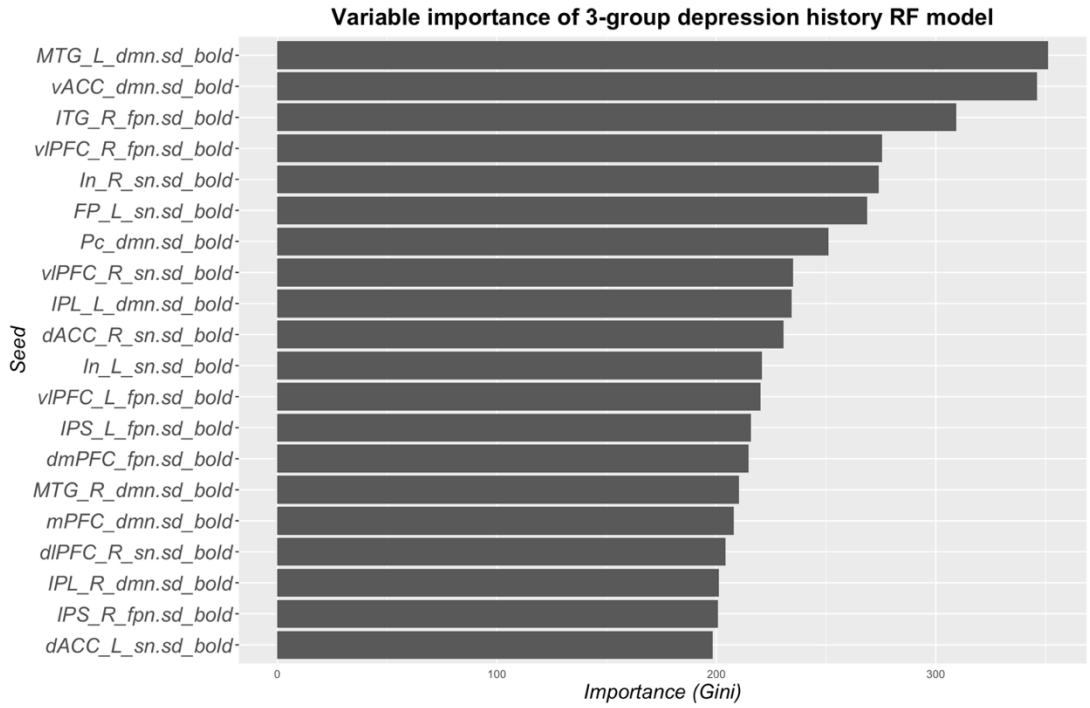

Figure 11. Variable importance plot depicting the Gini importance of the top 20 most important features from the 3-level depression history classification random forest (caret::varImp).

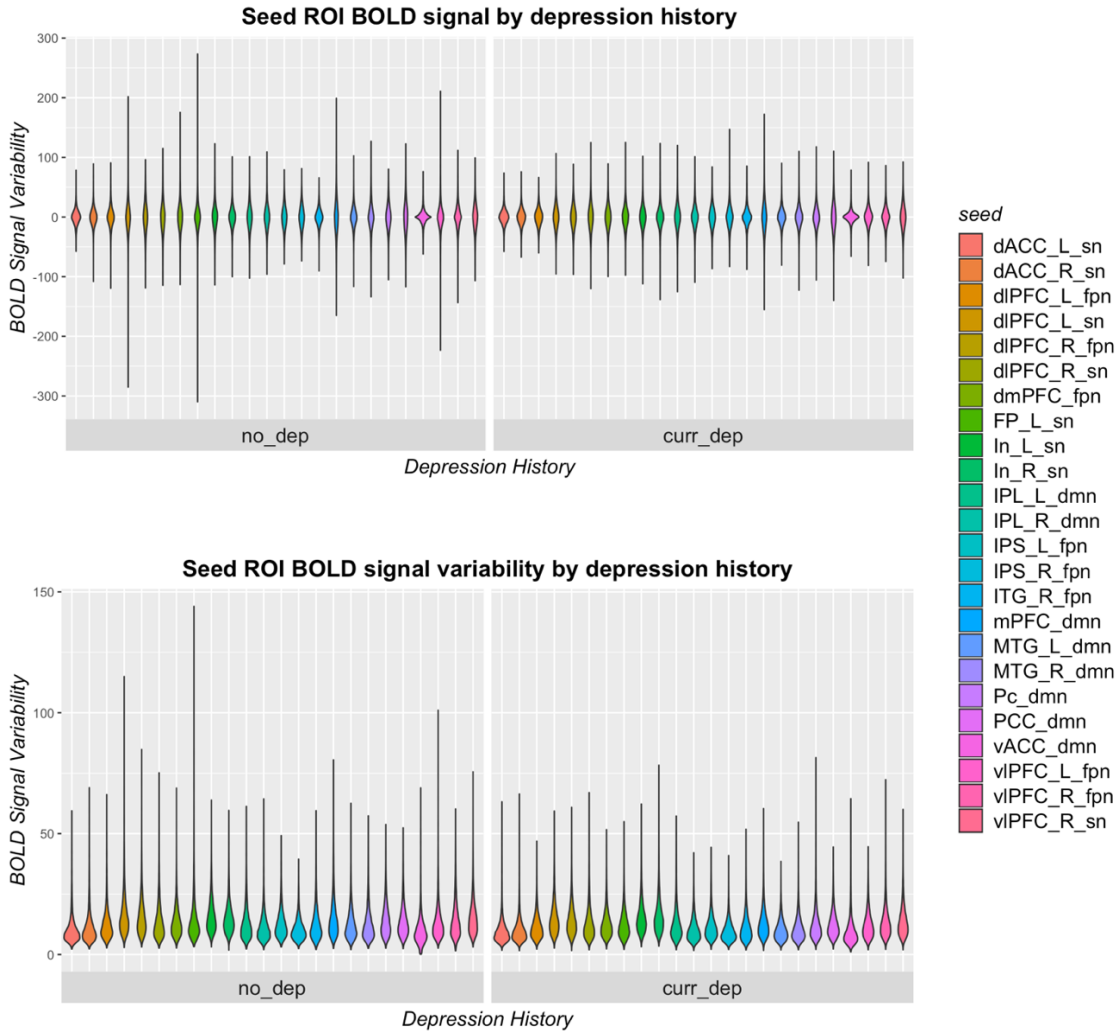

Figure 12. Violin plots illustrating the distribution of BOLD signal features (*top*) and BOLD signal variability features (*bottom*) within two levels of depression history.

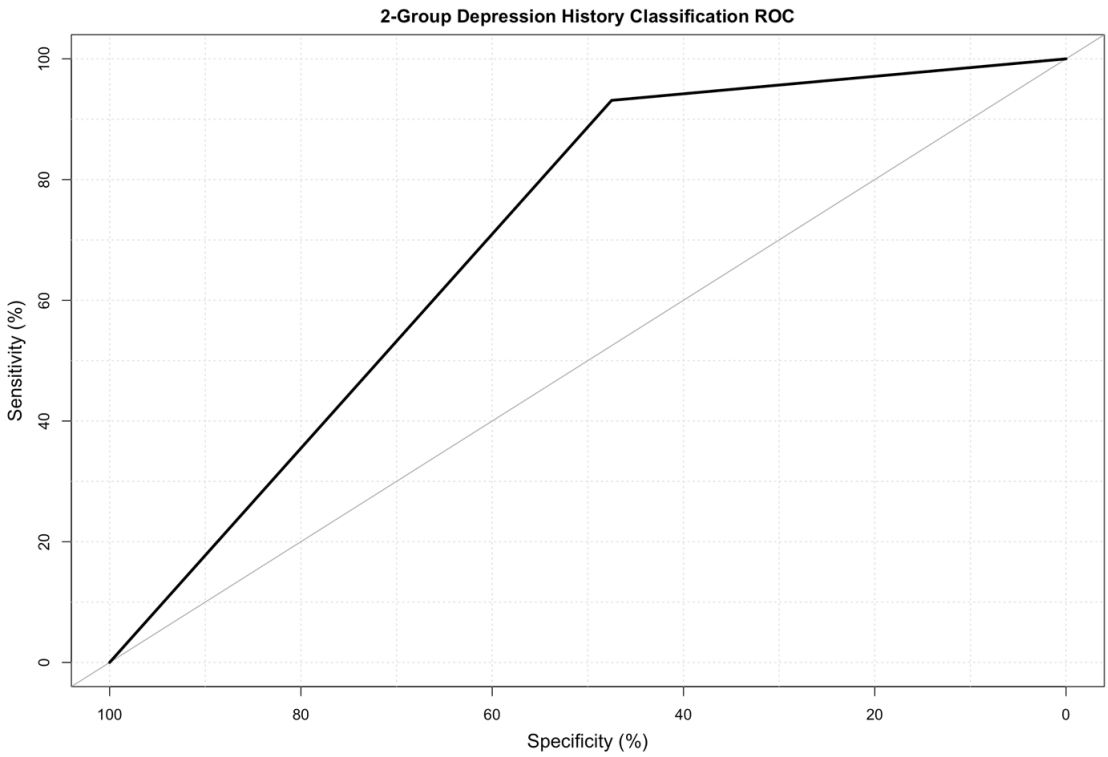

Figure 13. ROC curve for the 2-level depression history classification random forest.

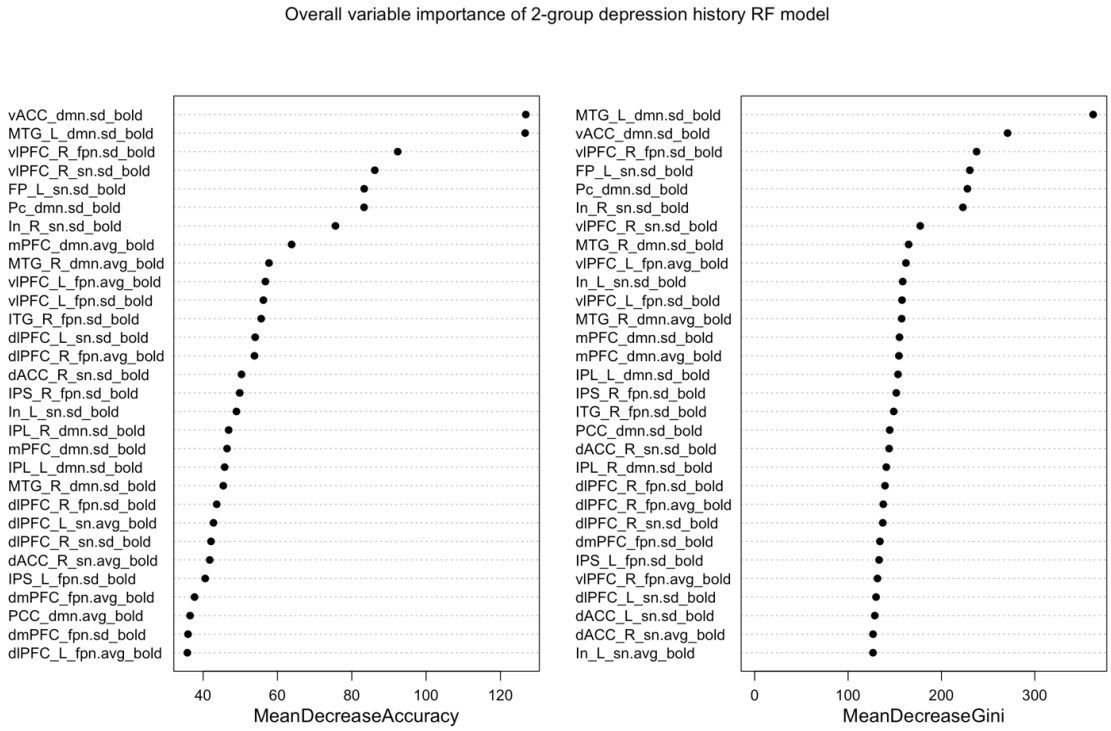

Figure 14. Variable importance plot including mean decrease in accuracy and Gini importance for the 2-level depression history classification random forest (randomForest::varImpPlot).

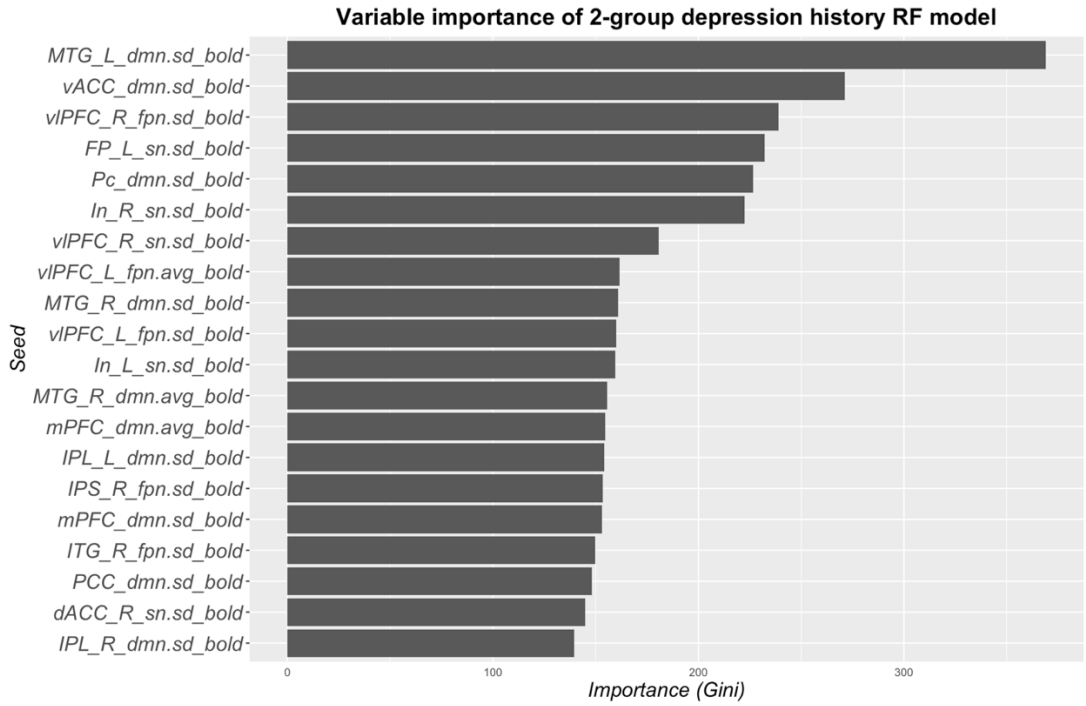

Figure 15. Variable importance plot depicting the Gini importance of the top 20 most important features from the 2-level depression history classification random forest (caret::varImp).

Tables

Table 1. Demographics by depression group

	NoDep (n = 30)	PastDep (n = 15)	CurrentDep (n = 34)
Age	27.1 (7.6)	28.0 (5.8)	27.9 (7.1)
Education Level			
High school diploma/equivalent	0	1	0
Some college, no degree	12	4	10
Associate's degree	1	1	1
Bachelor's degree	7	6	11
Master's degree	8	3	10
Doctoral degree	2	0	2
Race			
White	22	13	25
Asian	5	2	6
African American	3	0	1
Unknown	0	0	2
BDI-II – Placebo Day	0.93 (1.46)	1.33 (2.16)	20.26 (10.76)

Table 2. Resting-state networks ROI coordinates

DMN				**SN**				**FPN**			
ROI	*x*	*y*	*z*	ROI	*x*	*y*	*z*	ROI	*x*	*y*	*z*
Pc	-5	-62	48	In R	42	10	-12	dlPFC R	46	46	14
PCC	-5	-54	21	In L	-40	18	-12	dlPFC L	-34	46	6
vACC	3	36	-9	dACC R	6	22	30	IPS R	38	-56	44
IPL R	53	-29	23	dACC L	-6	18	30	IPS L	-48	-48	48
IPL L	-58	-38	28	FP L	-24	56	10	ITG R	58	-54	-16
mPFC	-2	53	21	vlPFC R	42	46	0	vlPFC R	34	56	-6
MTG R	45	-68	14	dlPFC R	30	48	22	vlPFC L	-32	54	-4
MTG L	-42	-68	16	dlPFC L	-38	52	10	dmPFC	0	36	46

MNI coordinates of resting-state network regions of interest. dACC, dorsal anterior cingulate cortex; dlPFC, dorsolateral prefrontal cortex; DMN, default mode network; dmPFC, dorsomedial prefrontal cortex; FP, frontal pole; FPN, frontoparietal network; In, insula; IPL, inferior parietal lobule; IPS, intraparietal sulcus; ITG, inferior temporal gyrus; MFG, middle frontal gyrus; mPFC, medial prefrontal cortex; MTG, middle temporal gyrus; Pc, precuneus; PCC, posterior cingulate cortex; ROI, region of interest; SN, salience network; vACC, ventral anterior cingulate cortex; vlPFC, ventrolateral prefrontal cortex.

Table 3. Results from Aim 1 analyses

Cluster location	MNI coordinates (x, y, z)	Cluster size	Test value
Full ANCOVA model			*F* value
R. cerebellum vermal lobule VIII	17, -63, -51	9	14.94*
L. cerebellum vermal lobule VIII	-19, -69, -51	7	11.79*
ANCOVA additional output: No history of depression vs. current depression			*t* value
R. cerebellum vermal lobule VIII	17, -63, -40	15	5.29*
L. cerebellum vermal lobule VIII	-19, -69, -54	10	4.69*
No history of depression vs. history of depression			*t* value
L. cerebellum vermal lobule VI extending to lobule VII	-7, -69, -24	89	5.07**
R. cerebellum vermal lobule VIII	12, -60, -51	48	5.44**
R. inferior parietal lobule extending to superior parietal lobule	32, -45, 54	40	4.53**

*Results at uncorrected threshold, $p < .001$.
**Results significant after family-wise error cluster correction, $p_{FWE} < .05$.

Table 4. Results from the Aim 2 multivariate linear multiple regression

Cluster location	MNI coordinates (x, y, z)	Cluster size	*t* value
R. cerebellum vermal lobule VIII	14, -69, -48	10	-3.74*
L. cerebellum vermal lobule VIII	-10, -63, -51	10	-3.98*

*Results at uncorrected threshold, $p < .001$.

Table 5. Confusion matrix for the 3-level depression history classification random forest

Confusion Matrix	*Reference*			Within Class Evaluation Metrics		
Prediction	NoDep	PastDep	CurrDep	*Sensitivity*	*Specificity*	*Accuracy*
NoDep	1612	48	815	69.75	79.48	74.62
PastDep	264	350	623	77.43	85.38	81.40
CurrDep	435	54	2316	61.69	82.30	72.00

Evaluation confusion matrix for RF classification of 3 levels of depression history. NoDep = no history of depression; PastDep = previous history of depression; CurrDep = current depression.

Table 6. Variable importance for the 3-level depression history classification random forest

Measure	ROI	MDA	Gini
Default Mode Network			
SD BOLD	MTG L	112.30	351.16
SD BOLD	vACC	110.30	346.12
SD BOLD	Pc	54.79	251.15
SD BOLD	IPL L	49.92	234.40
SD BOLD	MTG R	44.73	210.26
SD BOLD	mPFC	49.78	207.82
SD BOLD	IPL R	49.98	201.08
Salience Network			
SD BOLD	In R	78.52	273.91
SD BOLD	FP L	87.86	268.66
SD BOLD	vlPFC R	62.70	235.01
SD BOLD	dACC R	56.04	230.68
SD BOLD	In L	57.62	220.80
SD BOLD	dlPFC R	52.50	204.32
SD BOLD	dACC L	44.29	198.40
Frontoparietal network			
SD BOLD	ITG R	108.72	309.33
SD BOLD	vlPFC R	84.55	275.43
SD BOLD	vlPFC L	64.43	220.12
SD BOLD	IPS L	50.83	215.71
SD BOLD	dmPFC	63.80	214.74
SD BOLD	IPS R	42.10	200.65

Mean decrease in accuracy and Gini importance for the top 20 most important variables in the 3-level depression history RF classifier. AVG BOLD, average BOLD signal across seed voxels; dACC, dorsal anterior cingulate cortex; dlPFC, dorsolateral prefrontal cortex; dmPFC, dorsomedial prefrontal cortex; FP, frontal pole; Gini, Gini importance; In, insula; IPL, inferior parietal lobule; IPS, intraparietal sulcus; ITG, inferior temporal gyrus; MDA, mean decrease in accuracy; mPFC, medial prefrontal cortex; MTG, middle temporal gyrus; Pc, precuneus; PCC, posterior cingulate cortex; ROI, region of interest; SD BOLD, standard deviation of BOLD signal across seed voxels; ACC, ventral anterior cingulate cortex; vlPFC, ventrolateral prefrontal cortex.

Table 7. Confusion matrix for the 2-level depression history classification random forest

Confusion Matrix	*Reference*		Between Class Evaluation Metrics		
Prediction	NoDep	DepHist	*Sensitivity*	*Specificity*	*Accuracy*
NoDep	1176	1299	80.82	74.34	75.79
DepHist	279	3763			

Evaluation confusion matrix for RF classification of 3 levels of depression history. NoDep = no history of depression; PastDep = previous history of depression; CurrDep = current depression.

Table 8. Variable importance for the 2-level depression history classification random forest

Measure	ROI	MDA	Gini
Default Mode Network			
SD BOLD	MTG L	126.64	362.49
SD BOLD	vACC	126.83	270.85
SD BOLD	Pc	83.31	227.82
SD BOLD	MTG R	45.43	164.88
AVG BOLD	MTG R	57.72	157.42
SD BOLD	mPFC	46.43	155.08
AVG BOLD	mPFC	63.81	154.46
SD BOLD	IPL L	45.78	153.49
SD BOLD	PCC	28.57	144.57
SD BOLD	IPL R	46.87	140.94
Salience Network			
SD BOLD	FP L	83.34	230.38
SD BOLD	In R	75.61	223.00
SD BOLD	vlPFC R	86.19	177.28
SD BOLD	In L	48.96	158.55
SD BOLD	dACC R	50.32	143.95
Frontoparietal network			
SD BOLD	vlPFC R	92.36	237.67
AVG BOLD	vlPFC L	56.75	162.00
SD BOLD	vlPFC L	56.21	157.78
SD BOLD	IPS R	49.84	151.66
SD BOLD	ITG R	55.61	148.90

Mean decrease in accuracy and Gini importance for the top 20 most important variables in the 2-level depression history RF classifier. AVG BOLD, average BOLD signal across seed voxels; dACC, dorsal anterior cingulate cortex; dlPFC, dorsolateral prefrontal cortex; dmPFC, dorsomedial prefrontal cortex; FP, frontal pole; Gini, Gini importance; In, insula; IPL, inferior parietal lobule; IPS, intraparietal sulcus; ITG, inferior temporal gyrus; MDA, mean decrease in accuracy; mPFC, medial prefrontal cortex; MTG, middle temporal gyrus; Pc, precuneus; PCC, posterior cingulate cortex; ROI, region of interest; SD BOLD, standard deviation of BOLD signal across seed voxels; ACC, ventral anterior cingulate cortex; vlPFC, ventrolateral prefrontal cortex.